Measurements in a Self Preserving Plane Wall Jet in a Positive Pressure Gradient.

by

H.P.A.H. Irwin

M.E.R.L. Report No. 73-2

Mechanical Engineering Research Laboratories

McGill University

Montreal, Quebec, Canada

April 1973

Measurements in a Self Preserving Plane Wall Jet in a Positive Pressure Gradient

Summary

Measurements of a wall jet in a self preserving pressure gradient are described. The quantities measured with a linearized hot wire anemometer were mean velocity, the turbulence stresses, triple and quadruple velocity correlations, intermittency and spectra of the longitudinal turbulence intensity. The turbulence as well as the mean flow reached a self-preserving state in which the ratio of the maximum velocity to the free stream velocity was 2.65. Skin friction was also measured using the razor blade technique in the viscous sublayer and buffer region. The values of the constants in the logarithmic law of the wall are found to be similar to those in boundary layer and pipe flows. The skin friction coeefficient is slightly lower than is found for the wall jet in still air (Guitton (1970)) but close to the formula of Bradshaw and Gee (1962) for the wall jet in an external stream in zero pressure gradient.

A balance of the terms in the turbulence energy equation is presented and discussed. The shearing stress is not zero at the point of maximum velocity but is of opposite sign to that at the wall and hence the contribution of this stress to turbulence production is negative in the outer part of the boundary layer region. However, the total turbulence production remains positive because the contribution of the normal stresses is positive and slightly larger. The pressure-velocity gradient correlations are evaluated by difference from the Reynolds stress equations and are compared with the

theoretical model of Hanjalić and Launder (1972(b)). Agreement is quite good in the outer region of the wall jet. The above model is also compared with the triple velocity correlations and again found to be in fair agreement.

ACKNOWLEDGEMENTS

The author would like to thank Dr. B.G. Newman for many helpful discussions and Mr. Lek Ah Chai for his assistance in some of the data analysis. This work was supported by the Defence Research Board of Canada under Grant number 9551-12.

Table of Contents

Notation

b	height of slot
C_f	skin friction coefficient $\tau w/\frac{1}{2}\rho U_m^2$
C_s, C_{ϕ_1}, C_{ϕ_2}	constants in equations 21 and 22
e_1, e_2	instantaneous values of the fluctuating components of the two signals from a x-wire
f	velocity profile function, $\frac{U-U_e}{U_0}$, or frequency
g	non-dimensional turbulent kinetic energy, $\frac{1}{2}\frac{\overline{q^2}}{U_0^2}$
g_{ij} $i=1,2,3$; $j=1,2,3$	non-dimensional components of the Reynolds stress $\frac{\overline{u_i u_j}}{U_0^2}$
H	form parameter, δ^*/θ
h	height of razor blade cutting edge above surface
K	empirical constant in equation (12) or the constant factor in the -5/3 law for the inertial subrange
k	wave number, $\frac{2\Pi f}{U}$
L_ε	dissipation length scale, $\left(\frac{1}{2}\overline{q^2}\right)^{3/2}/\varepsilon$
m	exponent in expression for self preserving form of the external flow velocity
p	fluctuating part of the pressure
Q_L	velocity of the air escaping from the louvres in the roof of the working section
q	total turbulent velocity

U,V,W	mean velocity in the positive x,y,z directions
u,v,w	turbulent velocity in the positive x,y,z directions
U_e	mean velocity in the flow external to the wall jet
U_m	maximum mean velocity in the wall jet
U_0	$U_m - U_e$
U_J	jet velocity at the slot
u_τ	skin friction velocity $\sqrt{\frac{\tau_w}{\rho}}$
x,y,z	cartesian coordinates x downstream, y normal to the surface
x_0	distance of the virtual origin of the wall jet upstream of the slot
x^*, y^*	variables in razor blade formula for the skin friction, $\log_{10}\left[\frac{\Delta p\ h^2}{\rho\nu^2}\right]$ and $\log_{10}\left[\left(\frac{u_\tau h}{\nu}\right)^2\right]$ respectively
y_0	distance from the wall to the point in the outer part of the wall jet where $\frac{U-U_e}{U_0} = \frac{1}{2}$
y_m	value of y at maximum mean velocity in wall jet
β	self preservation parameter, $-\frac{\delta^*}{\gamma^2 U_e}\frac{dU_e}{dx}$
γ	u_τ/U_e
Δp	pressure difference
δ^*	displacement thickness $\int_0^\infty \left(1 - \frac{U}{U_e}\right) dy$

ε	rate of dissipation of turbulent kinetic energy per unit mass
η	non-dimensional coordinate y/y_0
θ	momentum thickness $\int_0^\infty \frac{U}{U_e}\left(1 - \frac{U}{U_e}\right) dy$
λ	microscale, $\sqrt{\frac{15\nu\ \overline{u^2}}{\varepsilon}}$
ν	kinematic viscosity
ρ	density
τ_w	shear stress at the wall
ϕ_{ij}	components of the spectrum function of $\overline{u_i u_j}$

Superscripts

over-bar denotes time average

prime denotes differentiation with respect to η

1. INTRODUCTION

The experiments described in this paper are concerned with a plane wall jet advancing into an adverse pressure gradient. Wall jets in an external stream have been studied on a number of occasions and stimulus for this research has been the usefulness of a wall jet as a means of preventing boundary layer separation. Possibly because of the practical implications much, although not all, of this research has been primarily aimed at developing empirical prediction methods and, as a result, there are not many instances where detailed turbulence measurements have been obtained. In the present work a particular case has been studied in detail experimentally with a view to providing more definitive data than has hitherto been available.

Under certain conditions the boundary layer equations can be reduced to ordinary differential equations and, following Townsend (1956(a), (b)), flows for which this occurs have been termed self preserving. The conditions for self preservation of turbulent wall jets in adverse pressure gradients were first given by Patel and Newman (1961) who assumed that the skin friction could be ignored. When the skin friction is ignored the conditions become similar to those for free jets which have been dealt with in detail, along with wakes, by Newman (1967) and Gartshore and Newman (1969). For self preserving flows the interpretation of experimental data and the development of theoretical models becomes greatly simplified and Patel (1962) and Gartshore (1965) exploited this in work on wall jets in adverse pressure gradients. A similar course has been followed in the present work, the pressure gradient being tailored to satisfy the conditions for self preservation which now include the effect of the skin friction.

The measurements in the present experiments include skin friction, mean velocity profiles, turbulence shear stress and intensities, spectra, dissipation rate, single point triple and quadruple velocity correlations and the intermittency. Using the data the terms in the equation for the kinetic energy of the turbulence with the exception of the pressure velocity correlation have been evaluated. The pressure velocity gradient correlations have been obtained by difference from the Reynolds stress equations assuming, in addition, that the flow is locally isotropic. The pressure velocity gradient correlations and the triple velocity correlations are compared with the model proposed by Hanjalić and Launder (1972(b)).

The measurements of the mean velocity near to the wall, which were made using a linearized hot wire anemometer, show that the values of the constants in the logarithmic law of the wall are similar to the conventional ones for boundary layer and pipe flows. This is consistent with the more recent measurements for the wall jet in still air (Guitton (1970)). The skin friction measurements are found to be quite well predicted by the formula proposed by Bradshaw and Gee (1962) which was based on their data for the wall jet with an external stream but no pressure gradient.

A feature of wall jets that has attracted considerable interest is that the point of zero shear stress does not coincide with the point of maximum velocity. In the present experiments the point of zero shear stress lies closer to the wall than the velocity maximum as is also found to be the case for the wall jet in still air (Guitton 1970). Erian and Eskinazi (1964) found that the opposite occurred in a weak wall jet in a positive pressure gradient. The physical explanation of these results appears to be that in wall jets such as that of Erian and Eskinazi where the jet excess velocity is not very large compared to that of the external flow the turbulence of the boundary layer region is more vigorous than in the outer layer and hence diffusion of boundary

layer properties into the outer layer takes place. For stronger wall jets, such as the present one, and for wall jets in still air the opposite occurs.

In the present experiments the value of $\frac{U_m}{U_e}$ was 2.65 (see fig. 1. for the meaning of the symbols) and the Reynolds number, $\frac{U_m Y_0}{\upsilon}$, varied from approximately 2.8×10^4 near the slot to 1.1×10^5 at the furthest downstream position. The main measurements were made in the region $60 < x/b < 260$ where both the mean velocity and the turbulence profiles were self preserving.

2. THEORY

2.1 Conditions for self preservation from the Momentum Equation

The concept of self preserving turbulent flows was introduced by Townsend (1956(a) and (b)) and his approach is followed here. The conditions for self preservation are obtained by assuming the velocity and turbulent stresses to be given by self preserving forms and substituting these into the boundary layer equations. The boundary layer equations for turbulent flow can be written, neglecting the viscous stress, as

$$\left.\begin{aligned} U\frac{\partial U}{\partial x} + V\frac{\partial U}{\partial y} + \frac{\partial(\overline{u^2}-\overline{v^2})}{\partial x} + \frac{\partial \overline{uv}}{\partial y} &= U_e\frac{dU_e}{dx} \\ \frac{\partial U}{\partial x} + \frac{\partial V}{\partial y} &= 0 \end{aligned}\right\} \quad (1)$$

where U_e is the velocity in the irrotational flow outside the wall jet. The forms for the velocity and turbulence stresses are assumed to be

$$\left.\begin{aligned} U &= U_e + U_o f(\eta) \\ \overline{uv} &= U_o^2 g_{12}(\eta) \\ \overline{u^2} &= U_o^2 g_{11}(\eta) \\ \overline{v^2} &= U_o^2 g_{22}(\eta) \end{aligned}\right\} \quad (2)$$

where U_0 is a velocity scale which is a function of x only, $\eta = y/y_0$ and y_0 is a length scale which is also a function of x only. In the present work the scales U_0 and y_0 are defined according to fig. (1). Substitution of the above forms into the boundary layer equations leads to (Newman (1967))

$$\left\{\frac{y_0}{U_0}\frac{\partial U_0}{\partial x}\right\}\left[f^2+2(g_{11}-g_{22})\right]\left\{\frac{y_0}{U_0}\frac{dU_eU_0}{dx}\right\}[f]$$
$$-\left\{\frac{1}{U_0}\frac{dU_ey_0}{dx}\right\}[\eta f'] \quad -\left\{\frac{1}{U_0}\frac{dU_0y_0}{dx}\right\}\left[f'\int_0^\eta f\,d\eta\right] \qquad (3)$$
$$-\left\{\frac{dy_0}{dx}\right\}[\eta(g_{11}'-g_{22}')]-g_{12}'=0$$

where primes denote differentiation with respect to y. It follows that if f, g_{12}, g_{11} and g_{22} are to be independent of x the terms in the curly brackets must be constants i.e., $\frac{dy_0}{dx}$, $\frac{U_0}{U_e}$ and $\frac{y_0}{U_0}\frac{dU_0}{dx}$ must be constants. Thus

$$y_0 \propto (x + x_0) \qquad (4)$$

and

$$U_e \propto (x + x_0)^m \qquad (5)$$

where x_0 is the distance of the hypothetical origin upstream of the slot and the exponent, m, depends on the ratio U_0/U_e. An equation for the exponent m can be obtained from the boundary conditions and by integration of equation (3) from $\eta = 0$ to ∞. The necessary boundary conditions are

$$\left.\begin{aligned} f(\infty) &= 0 \\ g_{12}(\infty) &= 0 \\ g_{12}(0) &= -u_\tau^2/U_0^2 \end{aligned}\right\} \qquad (6)$$

where u_τ is the skin friction velocity $\sqrt{\frac{\tau_\omega}{\rho}}$, τ_ω being the shear stress at the wall. It can be seen from equation (6) that if g_{12} is to be independent of x then u_τ/U_0 must be a constant i.e. the skin friction coefficient must be constant. Also, it is known from experiment and dimensional reasoning that near to a wall the velocity scale of the mean flow is u_τ so that again $\frac{u_\tau}{U_0}$ must be constant for true self preservation to be possible. Carrying out the integration of equation (3)

from $\eta = 0$ to ∞ and ignoring the normal stress terms the following expression for m is obtained

$$m = \frac{-1}{H\left(1+\frac{1}{\beta}\right)+2} \tag{7}$$

where $\beta = -\frac{\delta^*}{\gamma^2 U_e}\frac{dU_e}{dx}$, $\gamma = u_c/U_e$, $\delta^* = \int_0^\infty \left(1-\frac{U}{U_e}\right)dy$

$H = \delta^*/\theta$ and $\theta = \int_0^\infty \frac{U}{U_e}\left(1-\frac{U}{U_e}\right)dy$.

The parameter β, which is constant for a particular self-preserving flow, is the same as that used by Mellor & Gibson (1966) for boundary layers.

Summarizing, the necessary condition for self-preservation is that $U_e \propto (x + x_0)^m$ where m is given by equation (7) in which it has been assumed that $\frac{u_\tau}{U_e}$ is constant. In practise the skin friction coefficient decreases slightly with increasing x and Mellor & Gibson's analysis of self-preserving boundary layers, took some account of this. In the present work it is assumed that the Reynolds number is sufficiently high for the variation of u_τ/U_e to be unimportant.

When the skin friction is zero $|\beta| = \infty$ and so equation (7) reduces to

$$m = \frac{-1}{H + 2} \tag{8}$$

which is the expression for m in free turbulent flows, Newman (1967), which are symmetrical about $y = 0$. For free jets equation (8) shows that m ranges from $-\frac{1}{2}$ for a very strong jet ($H = 0$) to $-\frac{1}{3}$ for a very weak jet ($H = 1.0$). For wall jets in positive pressure gradients equation (7) shows that m will be more negative than for a free jet with the same value of H because β is negative.

2.2 The Reynolds stress and turbulence energy equations.

The Reynolds stress equations contain terms that account for the viscous dissipation of turbulent energy. It is assumed here that the dissipation occurs in a locally isotropic part of the spectrum. It is also assumed that the viscous transport terms may be neglected. With these assumptions and by application of the boundary layer approximation the Reynolds stress equations for two dimensional mean flow become

$$
\left.
\begin{aligned}
&\underbrace{\frac{D\overline{u^2}/2}{Dt}}_{A} - \underbrace{\overline{\frac{p}{\rho}\frac{\partial u}{\partial x}}}_{R} + \underbrace{\overline{u^2}\frac{\partial U}{\partial x} + \overline{uv}\frac{\partial U}{\partial y}}_{P} + \underbrace{\frac{\partial \overline{vu^2}/2}{\partial y}}_{DV} + \underbrace{\frac{\varepsilon}{3}}_{E} = 0 \\
&\underbrace{\frac{D\overline{v^2}/2}{Dt}}_{A} - \underbrace{\overline{\frac{p}{\rho}\frac{\partial v}{\partial y}}}_{R} + \underbrace{\frac{\partial \overline{pv}/\rho}{\partial y}}_{DP} - \underbrace{\overline{v^2}\frac{\partial U}{\partial x}}_{P} + \underbrace{\frac{\partial \overline{v^3}/2}{\partial y}}_{DV} + \underbrace{\frac{\varepsilon}{3}}_{E} = 0 \\
&\underbrace{\frac{D\overline{w^2}/2}{Dt}}_{A} - \underbrace{\overline{\frac{p}{\rho}\frac{\partial w}{\partial z}}}_{R} + \underbrace{\frac{\partial \overline{vw^2}/2}{\partial y}}_{DV} + \underbrace{\frac{\varepsilon}{3}}_{E} = 0 \\
&\underbrace{\frac{D\overline{uv}}{Dt}}_{A} - \underbrace{\overline{\frac{p}{\rho}\left(\frac{\partial u}{\partial y} + \frac{\partial v}{\partial x}\right)}}_{PS} + \underbrace{\overline{v^2}\frac{\partial U}{\partial y}}_{P} + \underbrace{\frac{\partial \overline{uv^2}}{\partial y}}_{DV} + \underbrace{\frac{\partial \overline{pu}/\rho}{\partial y}}_{DP} = 0
\end{aligned}
\right\} \quad (9)
$$

where $\frac{D}{Dt} \equiv U\frac{\partial}{\partial x} + V\frac{\partial}{\partial y}$ and ε is the dissipation rate per unit mass. The terms in these equations have been labelled in the following way; A ≡ advection, R ≡ redistribution amongst components of the Reynolds stress, P ≡ production, DV ≡ diffusion by velocity fluctuations, DP ≡ diffusion by pressure fluctuations, PS ≡ pressure strain correlation and E ≡ dissipation. Addition of the three equations for the normal stresses leads to the

equation for the kinetic energy of the turbulence

$$\underbrace{\frac{D\,\overline{q^2}/2}{Dt}}_{A} + \underbrace{\overline{uv}\frac{\partial U}{\partial y} + (\overline{u^2}-\overline{v^2})\frac{\partial U}{\partial x}}_{P} + \underbrace{\frac{\partial \overline{vq^2}/2}{\partial y}}_{DV} + \underbrace{\frac{\partial \overline{pv}/\rho}{\partial y}}_{DP} + \underbrace{\varepsilon}_{E} = 0 \qquad (10)$$

where $q^2 = u^2 + v^2 + w^2$ and the same labelling applies. It can be shown that the conditions found previously for a self-preserving form of the momentum equation also lead to self-preserving forms of the Reynolds stress and energy equations. For example, in the case of the turbulence energy equation if the following self-preserving forms are assumed

$$\frac{\overline{q^2}}{2} = U_o^2\, g(\eta)\,,$$

$$\frac{\overline{pv}}{\rho} + \frac{\overline{vq^2}}{2} = U_o^3\, h(\eta)\,, \qquad (11)$$

$$\varepsilon = \frac{U_o^3}{y_o}\, e(\eta)$$

then equation (10) can be written (Gartshore and Newman (1969))

$$\left\{\frac{y_o U_e}{U_o^2}\frac{dU_o}{dx}\right\}[2g] + \left\{\frac{y_o}{U_o}\frac{dU_o}{dx}\right\}[2gf] - \left\{\frac{1}{U_o}\frac{d\,y_o U_e}{dx}\right\}[1g']$$

$$- \left\{\frac{1}{U_o}\frac{dy_o U_o}{dx}\right\}\left[g'\int_0^1 f\,d\eta\right] + [f' g_{12}] + [h'] + [e]$$

$$+ \left\{\frac{y_o}{U_o}\frac{dU_e}{dx}\right\}[g_{11} - g_{22}] + \left\{\frac{y_o}{U_o}\frac{dU_o}{dx}\right\}[f(g_{11}-g_{22})] - \left\{\frac{dy_o}{dx}\right\}[(g_{11}-g_{22})\eta f'] = 0 \qquad (12)$$

It is found that if the conditions for self-preservation derived from the momentum equation are satisfied then the terms in the curly brackets in (12) are automatically constant and thus that equation (10) is of self-preserving form.

3. EXPERIMENTS

3.1 The wind tunnel and jet

The experiments were carried out in an open circuit blower-type wind tunnel which has been described by Wygnanski and Gartshore (1963). The tunnel is driven by a single stage centrifugal fan powered by an 18 Kwatt 3 phase constant-speed electric motor and the speed is controlled by variable inlet vanes. The turbulence level is reduced by a honeycomb and three removable screens in the settling chamber upstream of a 6:1 contraction. The screen arrangement used in the experiments is described in a subsequent section. The wall jet emanated from a 6.73 mm high slot with a 3.18 mm thick lip spanning the working section floor at the contraction exit as shown in fig. (2). The air for the jet was supplied by a 15 Kwatt centrifugal fan and its temperature could be adjusted to equal that of the wind tunnel air using a water cooled heat exchanger in the air supply from the fan. The jet velocity was controlled using a throttle between the fan and heat exchanger. Both the wind tunnel and slot air was filtered down to 0.5μ using American Air-Filter fibreglass filters. The blowing slot was basically the same as that described by Gartshore and Hawaleshka (1964) who took care to eliminate three dimensional irregularities in the flow. The working section, fig. (2), was 0.76 m wide by 0.43 m high and 2.3 m long. The pressure gradient was tailored using adjustable louvres in the roof as shown in fig. (2) and a perforated plate at the exit. The floor was plexiglass except for the final 0.76 m of the working section which was aluminium and had two streamwise rows of static pressure holes 17.8 cm on either side of the centre line. In each of the side walls, which consisted of 3 plexiglass windows set in wood, there were 6 mm wide vertical slots at .3, 1.08 and 1.86 m from the jet slot to allow the side wall boundary layers to bleed away.

3.2 Instrumentation

Pitot tube and hot wire traverses were carried out using a traverse gear mounted above the working section. The traverse gear was basically that designed and built by Fekete (1970) for his experiments and consisted of a lead screw driven by a synchro receiver which was wired to a transmitter. The transmitter was coupled to a mechanical counter from which the position was read. It was checked for accuracy and found to be accurate to within .03 mm over 10 cm. The probe position was 'zeroed' relative to the surface by a reflection technique to an estimated accuracy of .03 mm.

The hot wire equipment used for measuring turbulent shear and normal stresses consisted of standard DISA normal and inclined wires and a constant temperature DISA 55D01 control unit, a 55D10 linearizer and a 55D25 auxiliary unit. Root mean square voltages were measured using the circuit in a DISA 55D35 unit. The r.m.s. output and mean voltages were fed to an analogue scanner and digitized by a VIDAR 521 digital voltmeter which were both part of a central computer facility (GE/PAC 4020) described by Vroomen (1970). Integration times for mean voltages were 10 seconds and the r.m.s. circuit was set to a 3 second time constant, the output being sampled ten times at about 1 second intervals and then averaged. For triple and quadruple velocity correlations a DISA X-wire, modified according to the recommendation of Jerome, Guitton and Patel (1971) to avoid thermal wake interference, was used. Additional units identical to those already described were used for the second wire. Two 55A06 correlators were used, one to obtain sums and differences of instantaneous voltages and the other to measure correlation coefficients. Where squaring of instantaneous signals was necessary the squaring circuits of the 55D35 r.m.s. meters were employed. Measurements of the r.m.s. voltages were read directly from the meters and mean voltages on two Hewlett Packard 2212A V.F. converter/5216

electronic counter combinations. For the measurements of spectra a Brüel and Kjaer 2112 audio frequency spectometer was employed, having a range from 25 to 40,000 Hz. The spectrometer output was read on one of the DISA r.m.s. voltmeters which had its time constant set to 30 seconds for the measurements at the low frequency end of the spectrum.

Pressures were measured by a range of Statham unbonded strain gauge transducers the most sensitive having a range of 0 to 0.07 kN/m^2 and a 48 port scani valve facilitated switching amongst the static pressure holes located in the floor of the working section. The transducer outputs were read by the voltmeter in the central computer facility or by a V.F. converter/electronic counter combination. The pitot tube used for the traverses was cylindrical with an outside diameter of 0.725 mm and had internally sharpened lips to reduce its sensitivity to flow direction. To measure skin friction a 0.254 mm (±2%) thick razor blade was positioned over a static hole and held to the surface by a small piece of adhesive tape at each end. East (1966) has made a detailed calibration of razor blades attached to the surface magnetically and Foster, Irwin and Williams (1971) found that using adhesive tape in the above manner caused no discernable departures from East's calibration. A further check on the calibration is described in a subsequent section.

3.3. Flow conditions

Besides being self preserving the flow also had to be adequately two dimensional. Before setting the pressure gradient, therefore, a series of trials were carried out to eliminate three-dimensional disturbances from the wind tunnel screens of the kind described by Bradshaw (1963), and Patel (1964) from the slot or from irregular boundary layer transition upstream of the slot. The final arrangement of the screens consisted of one with $k \simeq 3$ followed by a 3.8 cm deep honeycomb with 6.3 mm cells, the two screens downstream of the honeycomb being removed. Boundary

layer transition was fixed by a 2.3 mm dia steel rod glued across the floor 8.5 cm upstream of the slot. No special adjustments of the slot were required. After the pressure gradient and wall jet velocity had been set measurements of the lateral variation of skin friction were made using a Preston tube and V.C. Patel's (1965) calibration at about 200 slot widths from the slot. The results are shown in fig. (3) and the variation can be seen to be less than about ±3% in the central 36 cm of the working section. Since skin friction is a sensitive indicator of irregularities of a three dimensional nature the flow was deemed to be adequately two dimensional. The free stream turbulence at the exit of the contraction was 0.5% at the speed of the experiments with the above screen arrangement.

The pressure gradient was set by an iterative technique. In order that the exponent m could be accurately estimated in advance a case was chosen that corresponded closely to one of those investigated by Patel and Newman (1961). This enabled H and β to be evaluated from their data and then m could be calculated using equation (7). The essence of the iterative technique was to assume that the velocity Q_L of the air escaping from between the louvres was given by

$$\tfrac{1}{2}\rho Q_L^2 = \Delta p + K \cdot \tfrac{1}{2}\rho U_e^2 \qquad (12)$$

where Δp was the local pressure difference between the working section interior and the laboratory, and K was an empirical constant. Starting with a guessed value for K of 1 the louvre positions required for a particular value of m could be calculated using equation (12) and the continuity condition. The value of m actually achieved enabled an improved value of K to be calculated and so on. The final

value of K was about 0.7 and incorporates the effect of entrainment into the jet as well as accounting for contraction of the flow between the louvres. The level of Δp was adjusted by blanking off a certain proportion of the perforated plate at the end of the working section (fig. 2) with adhesive tape. Further adjustment was possible by altering the angle to the vertical of the perforated plate, which was hinged along its bottom edge. This had the effect of changing the gap between the plate and the last of the slots in the roof of the working section. The final conditions were $\frac{U_0}{U_e} = 1.65$, $m = -0.448$ and the extent of the power law variation of U_e is shown in fig. (4). It was found impossible to obtain a power law variation for $x/b < 60$, where b was the slot height, and at the downstream end the power law region was terminated at $x/b \triangleq 260$ by an abrupt pressure rise associated with the flow at the end of the working section. The main measurements were carried out in the range $60 < x/b < 260$. The value of the form parameter H was 0.452 ($\pm$.005) in the self preserving region and β varied from -1.86 at $x/b = 82.2$ to -2.07 at $x/b = 248.0$, indicating a slight departure from the self preserving condition due to increasing Reynolds number. It is interesting to note that if skin friction is neglected, i.e. $|\beta| = \infty$, then equation (7) gives a value for m of -0.408 for $H = 0.452$ which is very different from the value -.448 actually required. The significance of a difference of this size can be seen when it is remembered that the total range of m for self preserving free jets is only $-.50 < m < -.33$.

3.4 Comments on the data.

The pitot tube measurements of mean velocity were corrected for turbulent intensity using the formula

$$\frac{U}{U_{UNC.}} = 1 - \frac{1}{2}\left(\frac{\overline{u^2} + \overline{w^2} - \overline{v^2}}{U^2}\right)_{UNC.} \qquad (13)$$

where the subscript unc. indicates uncorrected quantities. This formula includes the correction for the static pressure variation across the wall jet caused by the transverse turbulent intensity.

The hot wire data for U, $\overline{uv}$, $\overline{u^2}$, $\overline{v^2}$ and $\overline{w^2}$ was corrected for longitudinal cooling using Champagne, Sleicher and Wehrmann's (1967) correction, which depends on the wire aspect ratio, and for high intensity effects using Guitton's (1970) equations. Champagne et al's correction was checked by the author before the present experiments were commenced (Irwin (1971)). Guitton's corrections include correlations upto fourth order and in the present work assumptions did not have to be made for the third and fourth order correlations because all the necessary terms were measured. It transpired that, despite intensities of up to 20%, the corrections were small, always less than 5%, owing to near cancellation of many of the terms in the equations. Nevertheless they were applied since the third and fourth order correlations were available. The third and fourth order correlations themselves were not however corrected.

The correlations $\overline{vw^2}$, $\overline{v^2w^2}$ and $\overline{uvw^2}$ were measured by aligning the plane of the x-wire parallel to the flow at 45° to the plane of the x and y axes shown in fig. 1. With the assumption that correlations involving odd powers of w

were zero, as should be the case for two dimensional flow, the following relations can be obtained

$$\left.\begin{aligned}
&\overline{(e_1 - e_2)^3} \propto \overline{v^3} + 3\,\overline{vw^2} \\
&\overline{(e_1 - e_2)^4} \propto \overline{v^4} + 6\,\overline{v^2w^2} + \overline{w^4} = \overline{(v+w)^4} \\
&\overline{e_1^2(e_1 - e_2)^2} \propto A^2\,\overline{u^2(v+w)^2} + B^2\,\overline{(v+w)^4} + 2AB\,\overline{u(v+w)^3} \\
&\overline{(e_1^2 - e_2^2)^2} \propto \overline{u^2(v+w)^2}
\end{aligned}\right\} \qquad (14)$$

where e_1 and e_2 are the fluctuating components of the two wires and A and B are calibration constants. Once $\overline{v^3}$ had been measured with the cross wire in the x-y plane, $\overline{vw^2}$ could be calculated from the first relation (Wygnanski and Fiedler (1969) and Hanjalić and Launder (1972(a)) have also obtained $\overline{vw^2}$ in this way). Similarly, the measurements of $\overline{v^4}$ and $\overline{w^4}$ enabled $\overline{v^2w^2}$ to be calculated from the second relation. In the third relation $\overline{u^2(v+w)^2}$ and $\overline{(v+w)^4}$ were obtained directly from $\overline{(e_1^2-e_2^2)^2}$ and $\overline{(e_1-e_2)^4}$ allowing $\overline{u(v+w)^3}$ to be calculated. In two dimensional flow $\overline{u(v+w)^3} = \overline{uv^3} + 3\overline{uvw^2}$ so to obtain $\overline{uvw^2}$ it was necessary to measure $\overline{uv^3}$ which was achieved by measuring $\overline{e_1^2(e_1-e_2)^2}$ with the plane of the x-wire in the x-y plane. Since the three correlations were obtained in this indirect fashion their accuracy was rather low.

The razor blade measurements of skin friction were reduced using the calibration formula of East (1966)

$$y^* = -0.23 + 0.618\,x^* + 0.0165\,x^{*2}$$

where

$$y^* = \log_{10}\left[\left(\frac{u_\tau h}{\nu}\right)^2\right], \qquad x^* = \log_{10}\left[\frac{\Delta p h^2}{\rho \nu^2}\right] \qquad (15)$$

and Δp is the difference between the pressure measured at the static hole with the razor blade in position and with it removed and h is the height of the blade cutting edge above the surface. Since the blades were laid flush with the surface h was assumed to be half the blade thickness i.e. 0.127 mm. Care was taken to clean the surface thoroughly before attaching each blade because small particles of dust would have introduced large errors in h. The technique was checked by comparing razor blade measurements with those of a 1.577 mm diameter Preston tube, using the calibration of V.C. Patel (1965), in a zero pressure gradient boundary layer and the results which are shown in fig. (5) are in good agreement.

The zero pressure gradient boundary layer was produced by putting a solid roof into the working section and raising the floor so that it lay flush with the upper surface of the slot lip. The different levels of skin friction were obtained by varying the wind speed in the range of 6 to 40 m/s and using different x stations. The Preston tube and razor blade measurements were made at identical positions. In the wall jet experiments the values of $u_\tau h/\nu$ for the blades was less than 11 for $x/b > 140$, was 14.6 at $x/b = 82.2$ and was 21.0 at $x/b = 35.7$. Thus the measurements did not extend beyond the 'buffer' region and over most of the self preserving section of the flow they were within the viscous sublayer and should therefore have been insensitive to possible changes in the constants of the logarithmic law of the wall.

4. EXPERIMENTAL RESULTS

4.1. Mean Flow Data

The variations of $\frac{U_0}{U_e}$ and $\frac{U_\tau}{U_e}$ are shown in fig. (6). The value of $\frac{U_0}{U_e}$ was effectively constant and equal to 1.66 for

$\frac{x}{b} > 60$ and $\frac{u_\tau}{U_e}$, obtained from razor blade measurements at the static hole positions on either side of the working section centreline, decreased by about 5% over the range $60 < x/b < 260$. In fig. (7) the present skin friction results and those of Patel (1962) for the same experimental conditions are compared with empirical formulae for wall jets in zero pressure gradient. The formula which has most experimental support is that for the wall jet in still air. Guitton (1970) critically examined the available skin friction data for this case as well as carrying out careful measurements of his own and concluded that the data is reasonably well fitted by

$$C_f = 0.0315 \left(\frac{U_m y_m}{\nu}\right)^{-0.182} \qquad (16(a))$$

where $C_f = \tau_w / \frac{1}{2} \rho U_m^2$. This formula had originally been proposed for the still air case by Bradshaw and Gee (1962) but on the basis of less experimental evidence. Although (16(a)) agrees quantitively with the available still air data the precise dependence of C_f on Reynolds number is still rather uncertain because of the small Reynolds number range of the experiments, roughly $3\times10^3 < \frac{U_m y_m}{\nu} < 3\times10^4$. For the wall jet with an external stream in zero pressure gradient Bradshaw and Gee (1962) and Kruka and Eskinazi (1964) have proposed formulae of the same form as (16(a)) but with different constants, the constants of Kruka and Eskinazi depending on the jet velocity to free stream velocity ratio. McGahan (1965) proposed a different formula based on assumptions about the velocity profile, without recourse to measurements of skin friction. It can be seen in fig.(7) that the three proposals for the wall jet with an external stream do not agree with each other but that Bradshaw and Gee's is close to the present and Patel's data. McGahan's formula appears to be slightly less accurate. The formulae of Kruka and Eskinazi fail to approach the fairly well established results for the wall jet in still air as U_m/U_e

becomes large, the value of C_f being far too low, which implies that the experimental data on which they were based are inaccurate. Those of Bradshaw and Gee may have suffered from a lack of two-dimensionality but it seems likely that this was not too serious because their results for the still air wall jet, obtained from the same apparatus, agree well with subsequent more definitive data (Guitton 1970). On balance then it seems that the formula of Bradshaw and Gee (1962)

$$C_f = 0.026 \left(\frac{U_m y_m}{\nu} \right)^{-0.18} \qquad (16(b))$$

is the most reliable at present for the wall jet with an external stream in zero pressure gradient for low values of U_m/U_e. If (16(b)) does accurately represent the zero pressure gradient case then the closeness of the present and Patel's results to it in fig. (7) would suggest that the pressure gradient has little influence on the skin friction. However, this must remain a tentative conclusion until the value of the skin friction in the zero pressure gradient case is more firmly established.

Mean velocity profiles which were measured using hot wires at four stations in the region $60 < x/b < 260$ are shown in fig. (8) and it can be seen that the scales y_0 and U_0 produce a good collapse of the data. A few of the pitot tube measurements from one station are included to show the level of agreement with the hot wire data which can be seen to be good. In fig. (9) the inner layer is given in more detail and shows a trend towards higher values of $(U - U_e)/U_0$ at a given η as x increases. This can be attributed to the gradual decrease in u_τ/U_e. A conventional logarithmic plot of the hot wire results for mean velocity in the wall region is shown in fig. (10). The skin friction velocity was that read from a mean curve through the razor blade measurements. From the results of Wills (1963) it was deduced that the effect of heat loss from the wire to the wall was negligible within

the logarithmic region. Also shown in fig. (10) is the logarithmic law of the wall with the constants recommended by V.C. Patel (1965) for pipe flows

$$\frac{U}{u_\tau} = 5.5 \log_{10}\left(\frac{yu_\tau}{\nu}\right) + 5.45 \qquad (17)$$

The good agreement of the data in fig. (10) with (17) indicates that the values of the constants in the logarithmic law for the present wall jet are similar to those found in boundary layer and pipe flows. Guitton (1970) came to the same conclusion for the wall jet in still air on the basis of his own data and a selection of the most reliable data from other sources so that it seems likely that it is a general result for all wall jets. However, it appears that for the wall jet in still air the region of validity of the universal law is rather small, $30 < \frac{yu_\tau}{\nu} < 100$ according to Guitton. In some earlier papers on wall jets unusual values of the constants were reported e.g. Myers, Schauer and Eustis (1961), Bradshaw and Gee (1962), Patel (1962), Kruka and Eskinazi (1964), Alcaraz, Guillermet and Mathieu (1968). But examination of these cases reveals either that the data was very probably in error or that the unusual constants arose from the subjective choice of region in which the logarithmic law is assumed to apply. As an example of the latter Guitton (1970) found that the data of Alcaraz et al (1968) is consistent with (17) provided the region of validity of the logarithmic law is taken to be $30 < \frac{yu_\tau}{\nu} < 100$, rather than $40 < \frac{yu_\tau}{\nu} < 300$ as chosen by the original authors. A main source of error is the large lateral variation of skin friction which can occur unless care is taken to ensure that the flow is truly two dimensional. The magnitude of this effect was not fully appreciated in the earlier measurements and so they must be viewed with circumspection. A further source of error is inadequate displacement corrections to pitot tube readings, which Dickinson and Ozarapoglu (1969) found to have a significant effect on the values of the logarithmic

law constants deduced from the data.

The measured values of y_0 and y_m, the distance from the wall to the velocity maximum ~~respectively~~, are shown in fig. (11) together with $(U_0/U_j)^{-1/448}$. The pitot tube and hot wire results are in good agreement. The virtual origins for y_0 and U_0 were very close to each other but that for y_m was slightly further upstream. The rate of growth $\frac{dy_0}{dx}$ was 0·0436 which is almost identical to that found by Patel and Newman (1961) for the same $\frac{U_0}{U_e}$. The Reynolds number $\frac{U_0 y_0}{\upsilon}$ varied from 3.3×10^4 to 7.2×10^4 over the self preserving region.

4.2 Turbulent shear stress and intensities.

The shear stress and intensities measured at four stations are shown in figs. (12) to (15). The data was initially made non-dimensional using U_e as a velocity scale and the scales in the figures have been adjusted using the mean value of U_0/U_e in order to express the results in terms of U_0. The measurements show that the turbulence was in a closely self preserving state except for a slight tendency for the point of zero shear stress to occur at lower values of η as x increased. The latter effect is another manifestation of the weak Reynolds number dependency of the inner layer. The range of measured skin friction in the region of the traverses is shown in fig. (12) and it can be seen to be in good agreement with the $\overline{uv}$ data. The shear stress obtained from the momentum equation, including the normal stress terms, and the measured velocity profiles is also shown in fig. (12). The agreement at the wall is very good but there is a discrepancy of about 13% at the point of maximum $\overline{uv}$. It may be noted that neglect of the normal

stress terms would have reduced the latter to about 7%. Considering the severity of the adverse pressure gradient this order of discrepancy is considered to be quite good.

The main features of u^2, v^2, and w^2 in figs. (13) and (15) are that they all reach their maximum values at about the same position as the maximum shear stress. u^2 exhibits a minimum near the position of zero shear stress, w^2 is almost constant in the inner layer and $\overline{v^2}$ decreases monotonically from its maximum value to zero at the wall. Over most of the wall jet u^2 is the largest of the three intensities but, for $\eta > 2.0$, v^2 becomes slightly larger. The maximum value of $\sqrt{u^2}/U$ was about 20% and this occurred at $\eta \sim 1.3$.

4.3 Higher order correlations.

The triple velocity correlations are shown in fig. (16). The most interesting of these were vu^2, v^2, vw^2 and uv^2 since they occur in the diffusion terms in the boundary layer form of the Reynolds stress equations (9). The two others, u^3 and uw^2, disappear from the equations when the boundary layer approximation is applied. All the triple velocity correlations pass through zero in the range $0.7 < \eta < 0.8$ which is slightly nearer to the wall than the position of maximum uv. The skewness factors of u and v are shown in fig. (17). They vary in a similar manner to each other except in the inner layer and in the intermittent part of the outer layer. For $\eta < 0.8$ the skewness factors resemble very much those of Hanjalić and Launder (1972(a)) in their asymmetric channel flow, the skewness of u tending to be more negative than that of v and the two being of opposite sign to each other over a large proportion of the inner layer $.02 < \frac{y}{y_0} < .12$. The large values at the edge of the flow are attributed to the intermittency there.

The fourth order velocity correlations, which were measured for the purpose of making corrections for high intensity effects, are shown in fig. (18). The flatness factors are shown in fig. (19) and they can be seen to be close to the Gaussian value of 3.0 over a large part of the flow but rising to higher values in the intermittent region. The flatness factors of u and v are similar to those of Hanjalić and Launder's (1972(a)) channel flow for $\eta < 0.8$ except that those of the latter authors reach a peak value of about 4.0 near to the velocity maximum whereas a peak is not so discernable in the present results in that position.

4.4 Intermittency

The intermittency distribution was measured using a mirror-galvanometer chart recorder with a frequency response which was 3db down at 3Khz. The $\frac{\partial u}{\partial t}$ signal obtained from the differentiation circuit of one of the correlators was recorded. The results, which were obtained by visual observation of the records are shown in fig. (20). Gartshore (1965) measured the intermittency of several self preserving wall jets, the two closest to the present case having $\frac{U_0}{U_e}$ of 1.92 and 0.91. The points where the measured intermittency was $\frac{1}{2}$ for these two cases were at $\eta = 1.56$ and 1.43 respectively which gives an interpolated value of $\eta = 1.53$ for the present case. This compares with $\eta = 1.66$ measured in the present tests. The difference between these two results illustrates the degree of subjectivity which inevitably enters into the definition of intermittency, however it is measured.

The ratio $\left(\overline{u^4}/\overline{u^2}^2\right)_{\eta=.8} \Big/ \left(\overline{u^4}/\overline{u^2}^2\right)_{\eta>.8}$ is also plotted in fig. (20) and tends to take higher values than the intermittency for η greater than about 1.6. A similar effect was observed in the measurements of Wygnanski and Feidler (1969) where it was attributed to the velocity fluctuations in the irrotational flow.

4.5 Spectra and dissipation measurements.

The spectrum function $\phi_{ij}(k)$ of $\overline{u_i u_j}$ is defined such that

$$\int_0^\infty \phi_{ij}(k)dk = 1 \qquad (18)$$

where $k = \frac{2\Pi f}{U}$ and f is the frequency in Hz. Only ϕ_{11} was measured and this was done at a number of points across the wall jet at x/b = 194. A representative selection of the results are shown in fig. (21). In the outer layer a significant range of -5/3 law existed and, following Bradshaw (1967), it was used to obtain the dissipation rate. The same method was used in the inner layer, despite the lack of a clear -5/3 region, by drawing a tangent of the appropriate slope to the data. For this reason the measured dissipation was not very reliable for $\eta < .15$. The -5/3 law can be expressed as

$$\overline{u^2}.\ \phi_{11}(k) = K\ \varepsilon^{2/3}\ k^{-5/3} \qquad (19)$$

where K is a constant. There is some variation in the reported values of K which is partly due to the choice of convection velocity for calculating the wave number from frequency. Fortunately there is an indirect check on the calculated dissipation. The diffusion term in the energy equation, when obtained by difference from the other three terms, should integrate to zero across the flow. The value of K was therefore adjusted until this occurred and was found to be 0.45. This is in quite good agreement with Bradshaw and Ferris (1965), Grant, Stewart and Moilliet (1962) and with Pond, Stewart and Burling (1963). The value of the turbulence Reynolds number $\sqrt{\overline{u^2}}\ \lambda/\upsilon$, where $\lambda^2 = 15\upsilon\ \overline{u^2}/\varepsilon$, was about 400 at $\eta = 1.0$. This satisfies the condition of Bradshaw (1967) that $\sqrt{\overline{u^2}}\ \lambda/\upsilon$ be greater than 100 for an inertial subrange to exist.

An attempt was also made to measure the dissipation rate using the assumption of local isotropy

$$\varepsilon = 15\upsilon \overline{\left(\frac{\partial u}{\partial x}\right)^2} \qquad (20)$$

Invoking Taylor's hypothesis, $\overline{\left(\frac{\partial u}{\partial x}\right)^2}$ was approximated by $\frac{1}{U}\overline{\left(\frac{\partial u}{\partial t}\right)^2}$ and $\frac{\partial u}{\partial t}$ was obtained from one of the DISA correlators. It was found however that a correction of order 100% was required for the effect of finite wire length*. This, combined with the possible inaccuracy of Taylor's hypothesis, makes these measurements of doubtful validity and they are not presented here. However, it is worth mentioning that the dissipation rate measured in this way agreed to within 25% with the -5/3 law results when the finite wire length correction of Wyngaard (1969) was applied.

The microscale $\lambda = \sqrt{\frac{15\upsilon\ \overline{u^2}}{\varepsilon}}$ and the dissipation length $L_\varepsilon = \left(\frac{1}{2}\overline{q^2}\right)^{3/2}/\varepsilon$ are shown in fig. (22). Also shown is the value of L_ε within the turbulent fluid which was calculated using the measured intermittency assuming q^2 to be negligible in the irrotational fluid.

4.6 Energy balance.

In fig. (23) the various terms in the energy equation (10) are shown. The production and advection terms were obtained from mean curves drawn through the data from the four traverse positions in the self preserving region and a three point formula was used for differentiation. The production term, it may be noticed, does not change sign at the velocity maximum, $\eta \sim 0.22$, owing to the contribution of the normal stress term $(\overline{u^2}-\overline{v^2})\frac{\partial U}{\partial x}$ which is of the same order as $\overline{uv}\frac{\partial U}{\partial y}$ near to the velocity maximum. In comparison, Kacker and

*NOTE:- In the -5/3 law range of the measurements there was no significant effect of finite wire length, $\left(y_0/\ell_{WIRE}\right)$ being 60.

Whitelaw (1969) and Erian and Eskinazi (1964) found that, in essentially zero pressure gradient, the normal stress term did not prevent the production from changing sign. A check was made to see if the neglect of the slight changes in mean velocity and shear stress profiles due to Reynolds number effects had masked a region of 'negative' turbulence production but this was found not to be the case.

The dissipation rate is almost equal to the production everywhere except in the region around the velocity maximum $.05 < \eta < .6$. This is associated with a balance of the diffusion and advection terms for $\eta > 0.6$, and is due to the relative smallness of these terms when $\eta < 0.05$. A similar situation seems to exist in the inner and outer parts of self preserving boundary layers, Bradshaw (1966).

The measured diffusion due to the velocity fluctuations is quite close to the total diffusion obtained by difference. In principle the diffusion term involving the pressure fluctuations is the difference between the two but the level of precision of the measurements, particularly of the dissipation rate, renders such a result of doubtful accuracy except possibly near to the outer edge of the flow where the dissipation and production are small. It is interesting to observe, however, that for $\eta > 0.6$ the 'pressure' diffusion term so obtained varies in qualitatively the same way as that determined by Wygnanski and Feidler (1969) in their axisymmetric free jet.

4.7 The Reynolds stress equations.

Assuming local isotropy the terms in the Reynolds stress equations (9) were evaluated and are shown in figs. (24(a), (b), (c), (d)). The terms $\overline{\frac{p}{\rho}\frac{\partial u}{\partial x}}$, $\overline{\frac{p}{\rho}\frac{\partial v}{\partial y}}$, $\overline{\frac{p}{\rho}\frac{\partial w}{\partial z}}$ were found by difference and $\overline{\frac{p}{\rho}\left(\frac{\partial u}{\partial y}+\frac{\partial v}{\partial x}\right)}$ was obtained in the same way,

neglecting the diffusion term $\frac{\partial\, \overline{pu}/\rho}{\partial y}$. Experimental points are not shown in figs. (24) because nearly all the results are derived from mean curves drawn through the data and, in some cases, numerical differentiation of these curves. The pressure-velocity gradient correlations R and PS according to the model proposed by Hanjalić and Launder (1972(b)) are also shown in figs. (24). Their model extends that originally proposed by Rotta in 1951 (Rotta (1962)) and includes the interaction between the mean rate of strain and the turbulence. In two dimensional boundary layer flows the following expressions are assumed for the pressure-velocity gradient correlations.

$$\left.\begin{aligned}
\overline{\frac{p}{\rho}\frac{\partial u}{\partial x}} &= -C_{\phi_1}\left(\frac{\varepsilon}{\overline{q^2}}\right)\left(\overline{u^2}-\overline{q^2}/3\right)+\overline{uv}\frac{\partial U}{\partial y}\left(\frac{6+4C_{\phi_2}}{11}-\frac{\overline{u^2}}{\frac{1}{2}\overline{q^2}}C_{\phi_2}\right)\\
\overline{\frac{p}{\rho}\frac{\partial v}{\partial y}} &= -C_{\phi_1}\left(\frac{\varepsilon}{\overline{q^2}}\right)\left(\overline{v^2}-\overline{q^2}/3\right)-\overline{uv}\frac{\partial U}{\partial y}\left(\frac{4-12C_{\phi_2}}{11}+\frac{\overline{v^2}}{\frac{1}{2}\overline{q^2}}C_{\phi_2}\right)\\
\overline{\frac{p}{\rho}\frac{\partial w}{\partial z}} &= -C_{\phi_1}\left(\frac{\varepsilon}{\overline{q^2}}\right)\left(\overline{w^2}-\overline{q^2}/3\right)-\overline{uv}\frac{\partial U}{\partial y}\left(\frac{2-6C_{\phi_2}}{11}+\frac{\overline{w^2}}{\frac{1}{2}\overline{q^2}}C_{\phi_2}\right)\\
\overline{\frac{p}{\rho}\left(\frac{\partial u}{\partial y}+\frac{\partial v}{\partial x}\right)} &= -C_{\phi_1}\left(\frac{\varepsilon}{\overline{q^2}}\right)2\overline{uv}+\frac{\partial U}{\partial y}\left(\frac{1-3C_{\phi_2}}{55}\overline{q^2}-\frac{2-6C_{\phi_2}}{11}\overline{u^2}\right.\\
&\qquad\left.+\frac{8-2C_{\phi_2}}{11}\overline{v^2}-\frac{\overline{uv}^2}{\overline{q^2}}C_{\phi_2}\right)
\end{aligned}\right\}\quad(21)$$

where $C\phi_1$ and $C\phi_2$ are constants given as 2.8 and 0.45 respectively. The right hand sides of equations (21) were evaluated using measured quantities. The agreement for the three normal stress equations is seen to be quite good for $\eta > 0.3$ but there is room for improvement in the region of the velocity maximum. In the case of the shear stress

equation, fig. (24d), agreement is quite good at the velocity maximum as well as in the outer layer. Hanjalić and Launder also proposed a model for the triple velocity correlations which occur in the diffusion terms of the Reynolds stress equations and their expressions for these can be written

$$
\left.
\begin{aligned}
\overline{u^3} &= -C_s \tfrac{3}{2}\frac{\overline{q^2}}{\varepsilon}\,\overline{uv}\frac{\partial \overline{u^2}}{\partial y} \\
\overline{uv^2} &= -C_s \tfrac{1}{2}\frac{\overline{q^2}}{\varepsilon}\left(\overline{uv}\frac{\partial \overline{v^2}}{\partial y} + 2\overline{v^2}\frac{\partial \overline{uv}}{\partial y}\right) \\
\overline{uw^2} &= -C_s \tfrac{1}{2}\frac{\overline{q^2}}{\varepsilon}\,\overline{uv}\frac{\partial \overline{w^2}}{\partial y} \\
\overline{vu^2} &= -C_s \tfrac{3}{2}\frac{\overline{q^2}}{\varepsilon}\left(\overline{v^2}\frac{\partial \overline{u^2}}{\partial y} + 2\overline{uv}\frac{\partial \overline{uv}}{\partial y}\right) \\
\overline{v^3} &= -C_s \tfrac{3}{2}\frac{\overline{q^2}}{\varepsilon}\,\overline{v^2}\frac{\partial \overline{v^2}}{\partial y} \\
\overline{vw^2} &= -C_s \tfrac{1}{2}\frac{\overline{q^2}}{\varepsilon}\,\overline{v^2}\frac{\partial \overline{w^2}}{\partial y}
\end{aligned}
\right\} \qquad (22)
$$

where $C_s = 0.08$. Again using measured quantities to evaluate the right hand sides these expressions have been compared with the measured triple velocity correlations in fig. (16). In the case of vu^2, v^3 and vw^2 the agreement is fairly good except that the model correlations reached their maximum positive values somewhat further from the wall than the measured ones. The model u^3 and uw^2 are too small by a factor of at least 2 but these correlations do not occur in the boundary layer form of the Reynolds stress equations so this may not be very important. The agreement in the case of uv^2 could be described as fair, the model value being too small for $\eta > 1.0$ but close to experiment nearer to the wall.

In obtaining the simplified form of the Reynolds stress equations given by (9) it has been assumed that at high wave numbers where nearly all the dissipation occurs the turbulence is locally isotropic. Arguments which make this a reasonable assumption for sufficiently high turbulence Reynolds number have been described by Batchelor(1952) in a discussion of the conditions for the existence of a range of 'universal equilibrium'. However, precisely what constitutes a sufficiently high Reynolds number has not been established largely due to the difficulty of making accurate measurements at high wave numbers. The turbulence Reynolds number $\sqrt{\overline{u^2}}\,\lambda/\upsilon$ in the outer part of the wall jet was about 400 at x/b = 194. This represents an improvement on the value of approximately 130 of Champagne, Harris and Corrsin (1970) who also used the local isotropy assumption in obtaining the pressure velocity gradient correlations by difference from the Reynolds stress equations. The measurements of the latter authors indicated that the turbulence in their experiment was 'roughly isotropic' at high wave numbers which gives support to the use of the assumption of the local isotropy in the present case. Near to the wall, of course, the turbulence Reynolds number becomes much smaller than in the outer region and the assumption becomes invalid.

4.8 The position of zero shear stress.

In the present experiments the point of zero shear stress always remained closer to the wall than the velocity maximum which is also the case for the wall jet in still air (e.g. Guitton (1970)). At the velocity maximum $\overline{uv}$ has a positive value and fig. (24(d)) shows that the diffusion term in the transport equation of $\overline{uv}$ is responsible. An interpretation of this is that the diffusion of positive $\overline{uv}$ towards the velocity maximum from the outer layer dominates that of negative $\overline{uv}$ from the inner layer. The data of Erian and Eskinazi (1964) is interesting in this context because it shows that in a weak wall jet this situation can be reversed. The reason for this appears to be that in a weak wall jet the turbulence level in the boundary layer region becomes higher than in the outer region as is evident in Erian and Eskinazi's data.

5. CONCLUSIONS

The following conclusions may be drawn from the present experiments:-

(a) It is possible to set up a wall jet in streaming flow that is closely self preserving both in the mean flow and the turbulence.

(b) The mean velocity profile in the region close to the wall was logarithmic with constants which were similar to the conventional values found in boundary layers and pipe flows.

(c) The skin friction formula of Bradshaw and Gee (1962) for wall jets in an external stream with zero pressure gradient agreed well with the measured skin friction.

(d) The absolute values of the rates of dissipation and production of turbulent kinetic energy were almost equal except near to the velocity maximum. This observation is associated with the near cancellation of the advection and diffusion terms in the outer layer and with the smallness of these terms in the inner region.

(e) The production of turbulence kinetic energy did not become negative near to the velocity maximum because in this region the normal stress production term was positive and of the same order as the negative shear stress term. The point of zero shear stress was, however, always closer to the wall than the velocity maximum.

(f) The model proposed by Hanjalić and Launder (1972(b)) for pressure velocity gradient correlations is in quite good agreement with experiment in the outer layer but agreement is not so good near to the velocity maximum. The important triple velocity correlations were modelled fairly well over most of the wall jet.

(g) The value of the constant factor in the -5/3 law for the inertial subrange was found to be 0.45.

References

Alcaraz, E., Guillermet, G. and Mathieu, J. (1968) 'Mesures de frottement à la paroi à l'aide de tube de Preston et d'une balance C.R.', Acad. Sc. Paris, t 266 Serie A, 432.

Batchelor, G.K. (1952) 'The theory of homogeneous turbulence', Cambridge University Press.

Bradshaw, P. and Gee, M.T. (1962) 'Turbulent wall jets with and without an external stream', Aero. Res. Counc. R & M No. 3252.

Bradshaw, P. (1963) 'The effect of wind tunnel screens on "two-dimensional" boundary layers', N.P.L. Aero Rep. 1085.

Bradshaw, P. and Ferris, D.H. (1965) 'The spectral energy balance in a turbulent mixing layer', Aero. Res. Counc. C.P. 899.

Bradshaw, P. (1966) 'The turbulence structure of equilibrium boundary layers', J. Fluid Mech. 29, 625.

Champagne, F.H., Sleicher, C.A. and Wehrmann, O.H. (1967) 'Turbulence measurements with inclined hot wires - Part I', J. Fluid Mech. 28, 153.

Champagne, F.H., Harris, V.G. and Corrsin, S. (1970) 'Experiments in nearly homogeneous turbulent shear flow', J. Fluid Mech. 41, 81.

Dickinson, J. and Ozarapoglu, V. (1969) 'The determination of turbulent skin friction', Progress Report, Dept. de Genie Mécanique, Université Laval.

East, L.F. (1966) 'Measurement of skin friction at low subsonic speeds by the razor-blade technique', Royal Aircraft Est. Tech. Rep. No. 66277.

Erian, F. and Eskinazi, S. (1964) 'The wall-jet in a longitudinal pressure gradient', Syracuse University Res. Inst., Mech. and Aerospace Eng. Dept. Rep. No. ME937-6410F.

Fekete, G.I. (1970) 'Two-dimensional, self-preserving turbulent jets in streaming flow', Mech. Eng. Res. Lab. Rep. 70-11, McGill University.

Foster, D.N. Irwin, H.P.A.H. and Williams, B.R. (1971) 'The two-dimensional flow around a slotted flap', Aero. Res. Counc. R & M No. 3681.

Gartshore, I.S. and Hawaleshka, O. (1964) 'The design of a two-dimensional blowing slot and its application to a turbulent wall jet in still air', Mech. Eng. Res. Lab. Tech. Note 64-5, McGill University.

Gartshore, I.S. (1965) 'The streamwise development of two-dimensional wall-jets and other two-dimensional turbulent shear flows', Ph.D. Thesis, McGill University.

Gartshore, I.S. and Newman, B.G. (1969) 'Small perturbation jets and wakes which are approximately self-preserving in a pressure gradient', C.A.S.I. Trans. 2, No. 2, 101.

Grant, H.L., Stewart, R.W. and Moilliet, A. (1962) 'Turbulence spectra from a tidal channel', J. Fluid Mech. 12, 241.

Guitton, D.E. (1970) 'Some contributions to the study of equilibrium and non-equilibrium wall jets over curved surfaces', Ph.D. Thesis, McGill University.

Hanjalić, K. and Launder, B.E. (1972(a)) 'Fully developed asymmetric flow in a plane channel', J. Fluid Mech. 51, 301.

Hanjalić, K. and Launder, B.E. (1972(b) 'A Reynolds stress model of turbulence and its application to thin shear flows, J. Fluid Mech. 52, 609.

Irwin, H.P.A.H. (1972) 'The longitudinal cooling correction for wires inclined to the prongs and some turbulence measurements in fully developed pipe flow', Mech. Eng. Res. Lab. Tech. Note 72-1, McGill University.

Jerome, F.E., Guitton, D.E. and Patel, R.P. (1971) 'Experimental study of the thermal wake interference between closely spaced wires of a X-type hot wire', Aero. Quarterly Vol. XXII, 119.

Kacker, S.C. and Whitelaw, J.H. (1969) 'The turbulence characteristics of two-dimensional wall jet and wall wake flows', Dept. Mech. Eng. Rep. BL/TN/6, Imperial College of Science and Technology.

Kruka, V. and Eskinazi, S. (1964) 'The wall jet in a moving stream', J. Fluid Mech. 20, 555.

McGahan, W.A. (1965) 'The incompressible turbulent wall jet in an adverse pressure gradient', Gas Turbine Lab. Rep. No. 82, Mass. Inst. of Technology.

Mellor, G.L. and Gibson, D.M. (1966) 'Equilibrium turbulent boundary layers', J. Fluid Mech. 24, 225.

Myers, G.E., Schauer, J.J. and Eustis, R.H. (1961) 'The plane turbulent wall jet. Part I - Jet development and friction factor;', Dept. Mech. Eng. Tech. Rep. No. 1, Stanford University.

Newman, B.G. (1967) 'Turbulent jets and wakes in a pressure gradient', Fluid Mechanics of Internal Flow. Gen. Motors Conf., Elsevier Publ. Co., Amsterdam.

Patel, R.P. and Newman, B.G. (1961) 'Self-preserving, two-dimensional turbulent jets and wall jets in a moving stream', Mech. Eng. Res. Lab. Rep. No. Ae 5, McGill University.

Patel, R.P. (1962) 'Self-preserving, two dimensional turbulent jets and wall jets in a moving stream', M.Sc. Thesis, McGill University.

Patel, R.P. (1964) 'The effects of wind tunnel screens and honeycombs on spanwise variation of skin friction in "two-dimensional" turbulent boundary layers. Mech. Eng. Res. Lab., Tech. Note 64-7. McGill University.

Patel, V.C. (1965) 'Calibration of the Preston tube and limitations on its use in pressure gradients', J. Fluid Mech. 23, 185.

Pond, S., Stewart, R.W. and Burling, R.W. (1963) 'Turbulence spectra in the wind over waves', J. Atmos. Sci. 20, 319.

Rotta, J.C. (1962) 'Universal aspects of the mechanism of turbulent boundary layer flow', Progress in Aero. Sciences Vol. 2, 22, MacMillan Co., New York.

Townsend, A.A. (1956(a)) 'The properties of equilibrium boundary layers', J. Fluid Mech. 1, 561.

Townsend, A.A. (1956(b)) 'The structure of turbulent shear flow', Cambridge University Press.

Vroomen, L.J. (1970) 'Data logger operating subsystem', Mech. Eng. Res. Lab., Memo 70-1, McGill University.

Wills, J.A.B. (1963) 'Note on a method of measuring skin friction', Nat. Phys. Lab. Aero. Note 1011.

Wygnanski, I. and Garshore, I.S. (1963) 'General description and calibration of the McGill 17 in. x 30 in. Blower Cascade Wind Tunnel', Mech. Eng. Res. Lab., Tech. Note 63-7, McGill University.

Wygnanski, I. and Feidler, H. (1969) 'Some measurements in the self-preserving jet', J. Fluid Mech. 38, 577.

Wyngaard, J.C. (1969) 'Spatial resolution of the vorticity meter and other hot-wire arrays', J. Sci. Instr. Series 2, 2, 983.

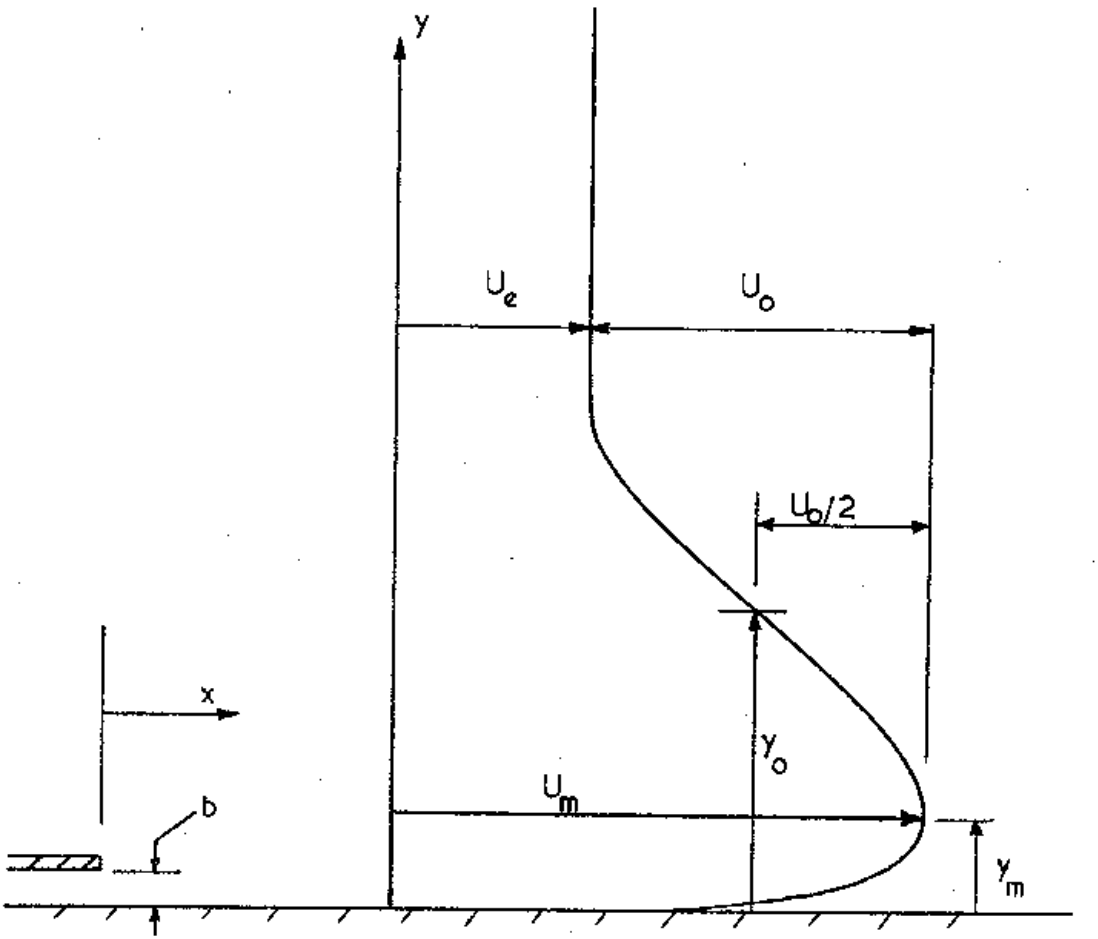

Fig. 1. Wall Jet Notation.

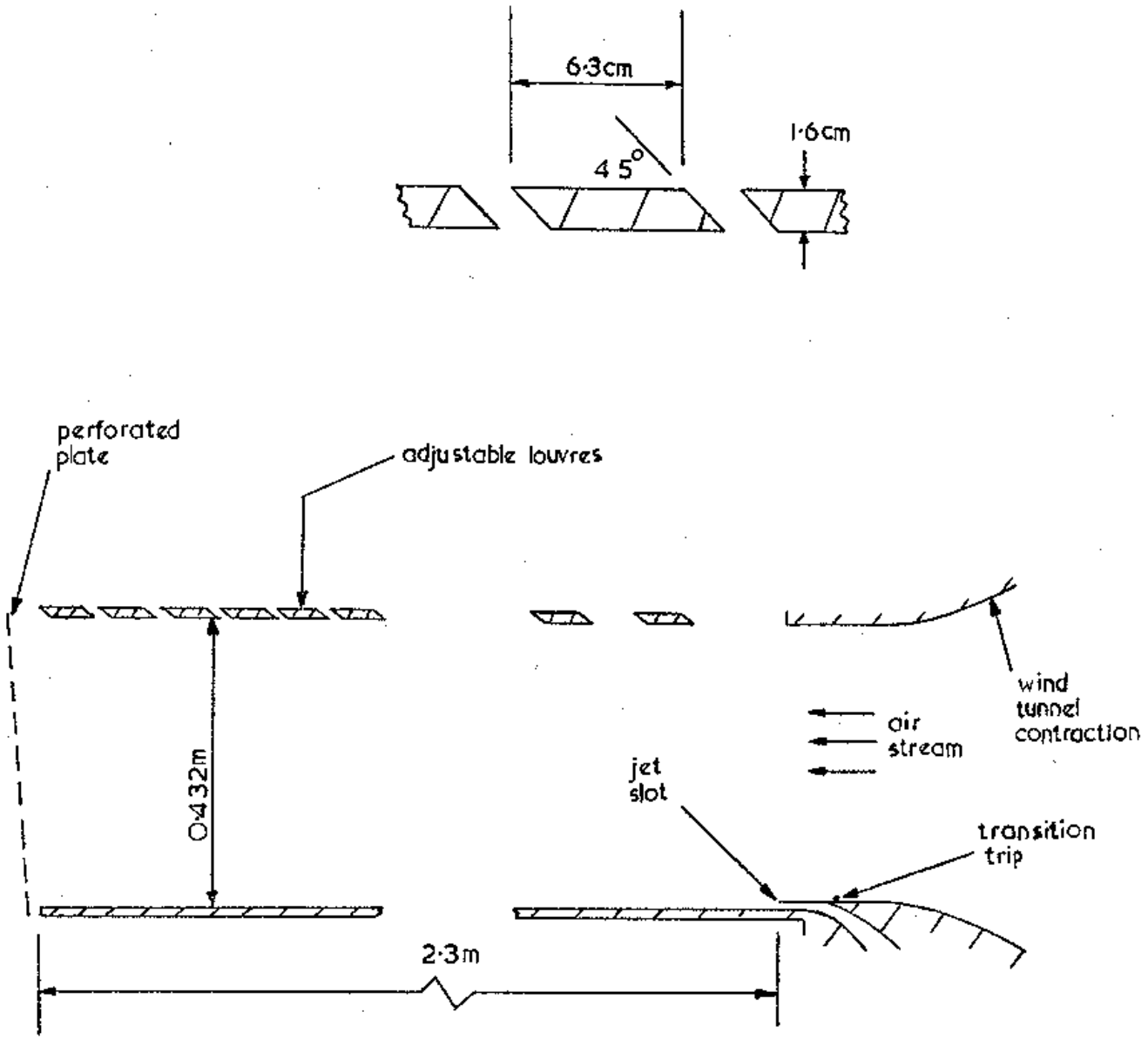

Fig. 2. Schematic Diagram of Working Section.

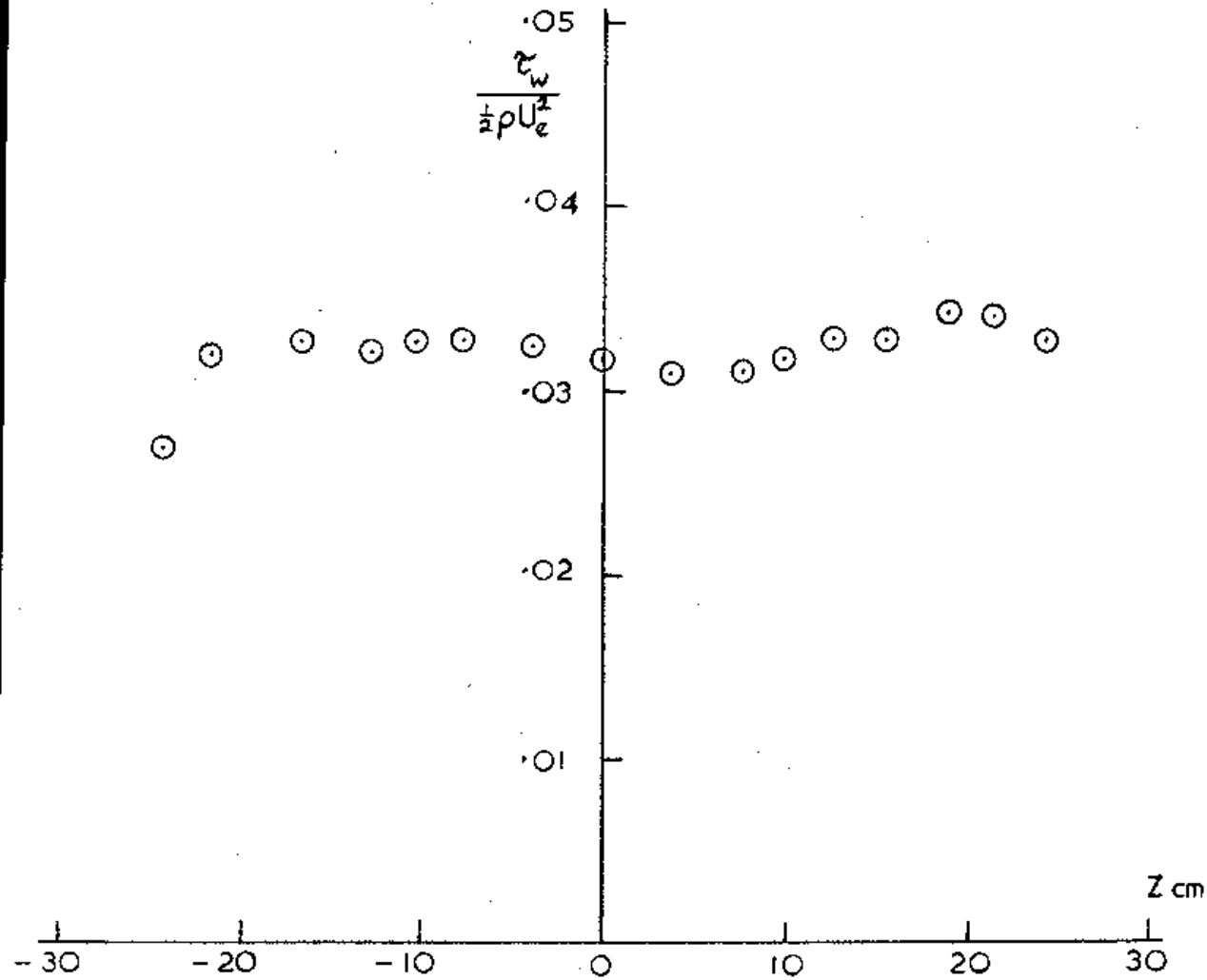

Fig. 3. Lateral Variation of Skin Friction at x/b = 200.

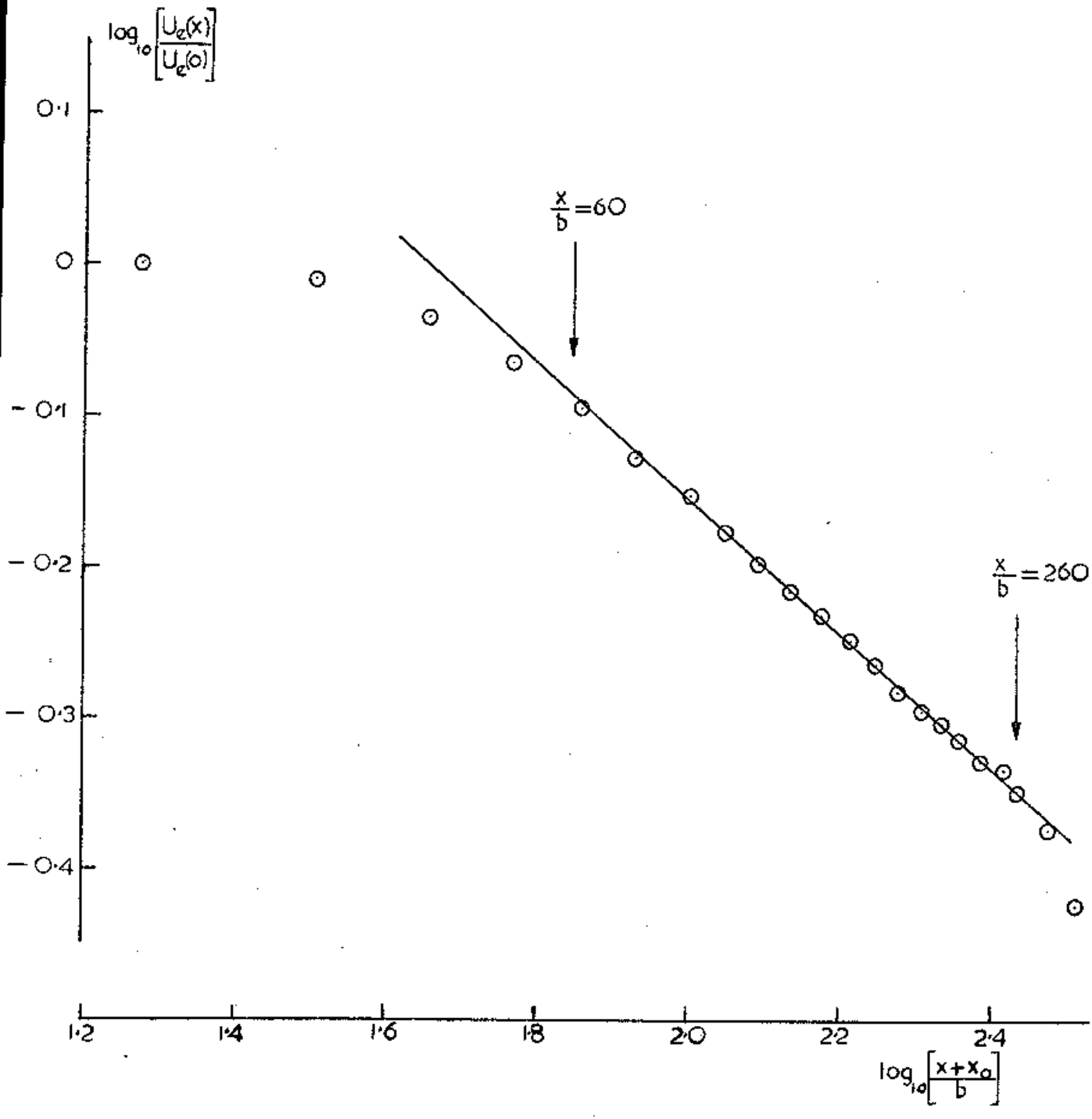

Fig. 4. Power Law Variation of External Flow Velocity.

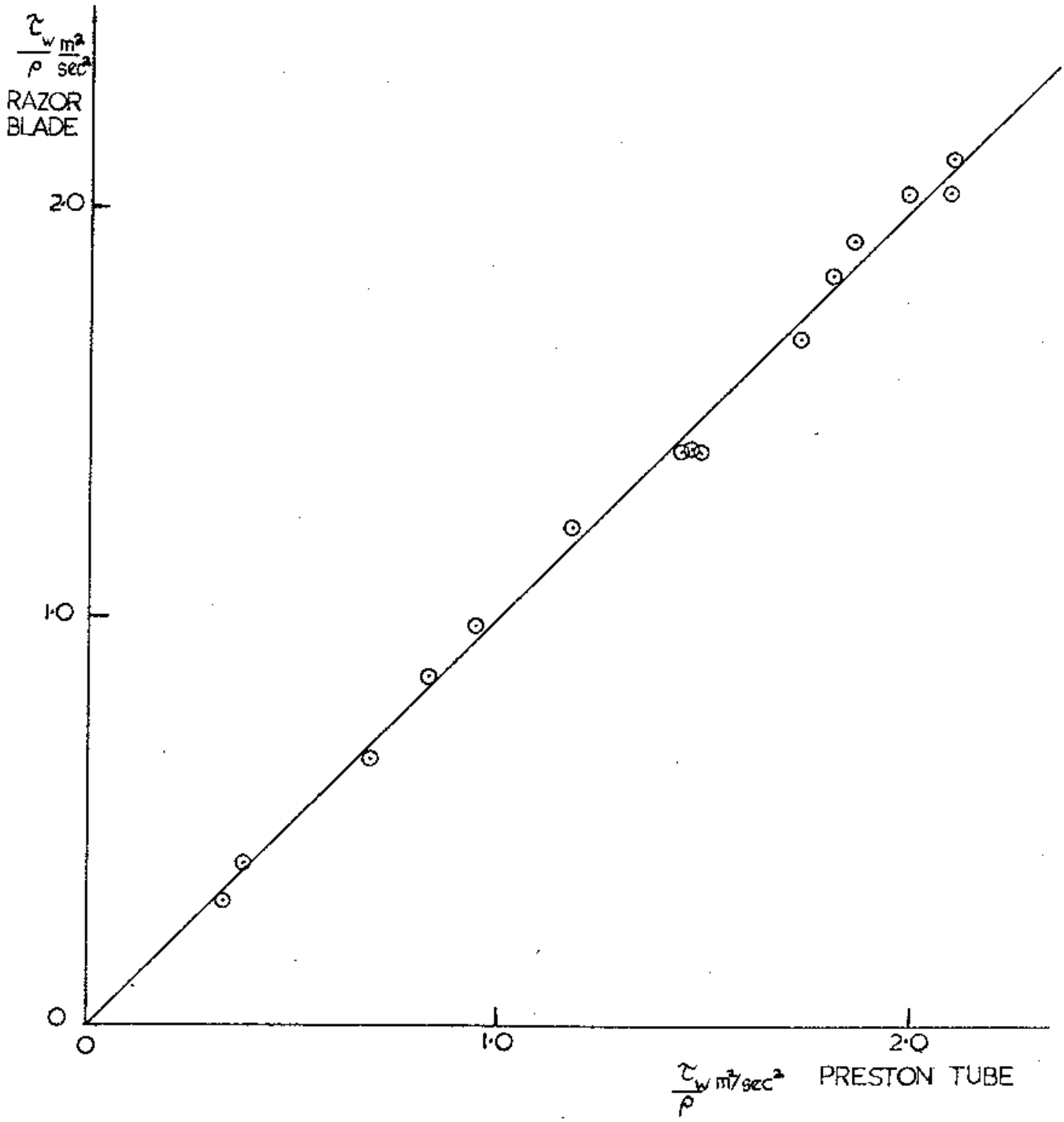

Fig. 5. Comparison of Razor Blade and Preston Tube Measurements of Skin Friction in a Zero Pressure Gradient Boundary Layer. ⊙ Measurements, ——— τ_w Razor Blade = τ_w Preston Tube.

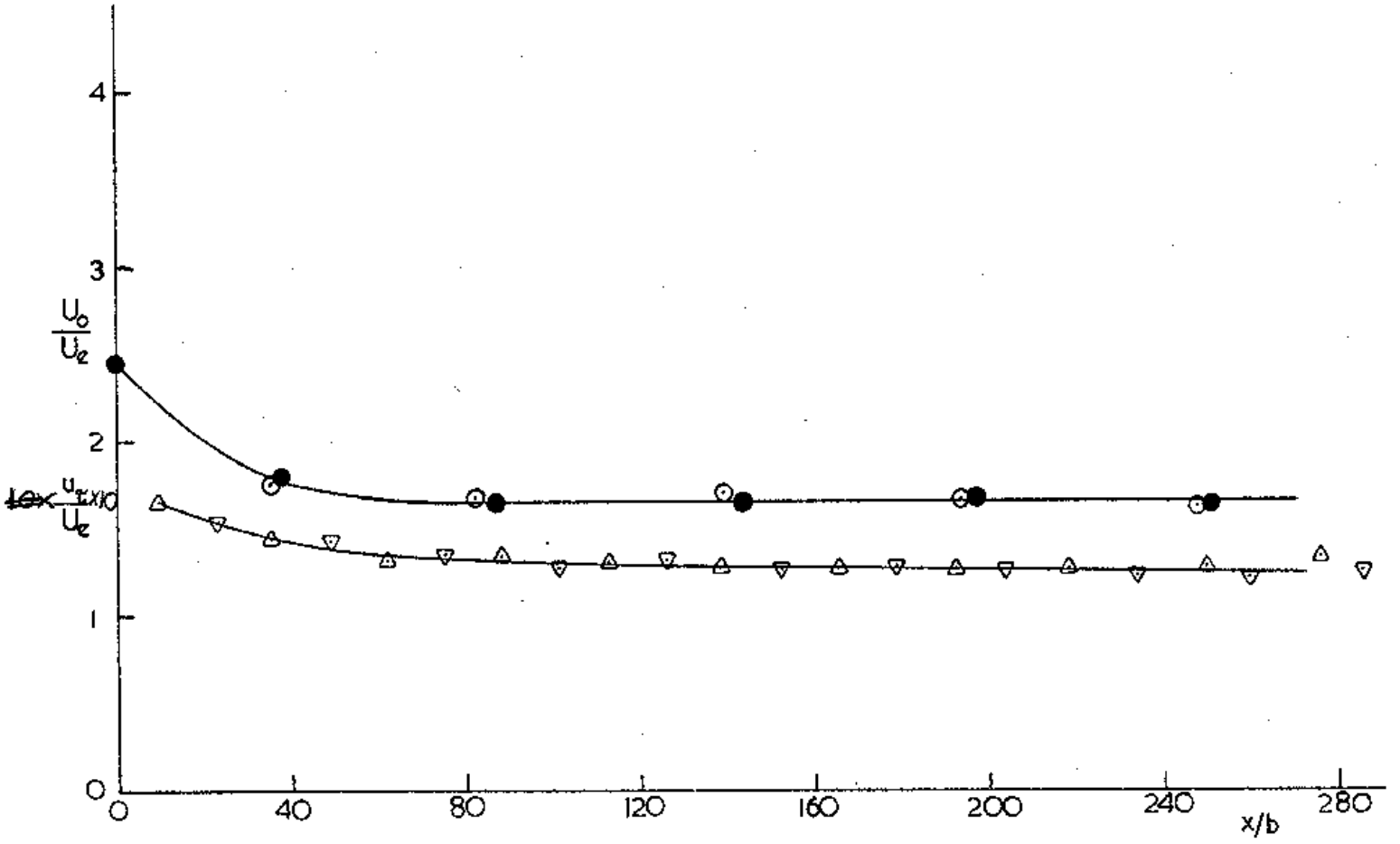

Fig. 6. Variation of U_0/U_e and U_τ/U_e. ● Pitot Tube, ⊙ Hot Wire U_0/U_e; △ , ▽ Razor Blade Measurements of U_τ/U_e at 17.8 cm on Either Side of the Centre-line of the Working Section.

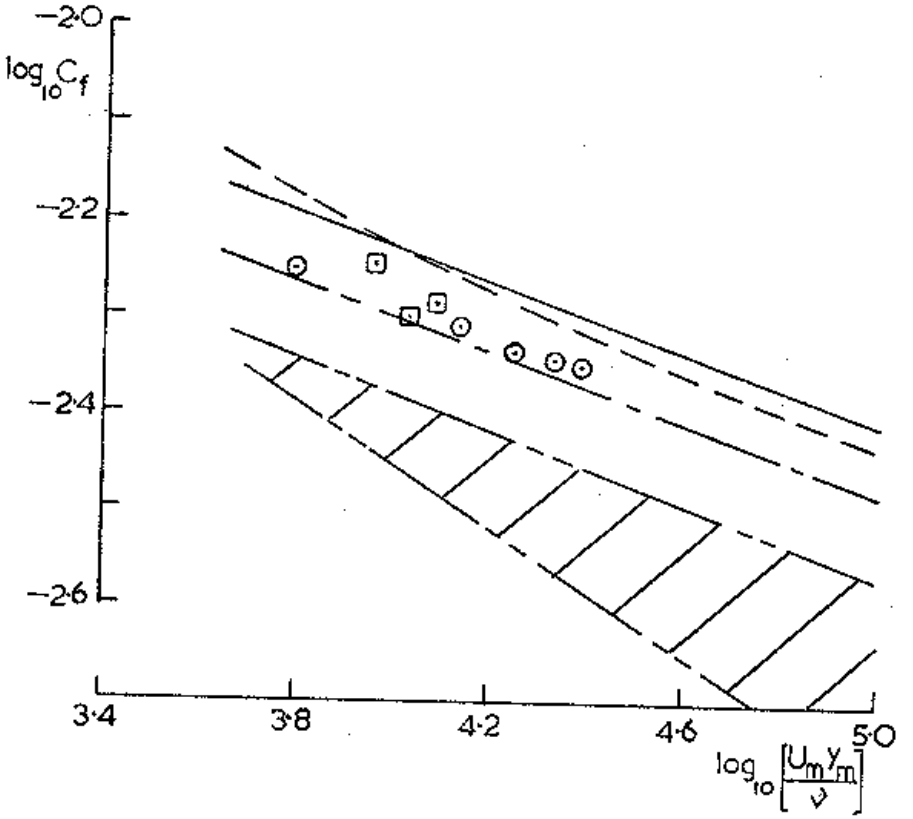

Fig. 7. Comparison of Skin Friction with Empirical Laws for Wall Jets in Zero Pressure Gradient. ⊙ Present Data, △ Data of Patel (1962): For Wall Jet in Still Air ———— Guitton (1970): For Wall Jet in External Stream —— — —— Bradshaw and Gee (1962) (Equation 16(b) $1 < U_m/U_e < 2$), Shaded Region Kruka and Eskinazi (1964) ($1.2 < U_m/U_e < 14$), ---- McGahan (1965) ($1.05 < U_m/U_e < \infty$).

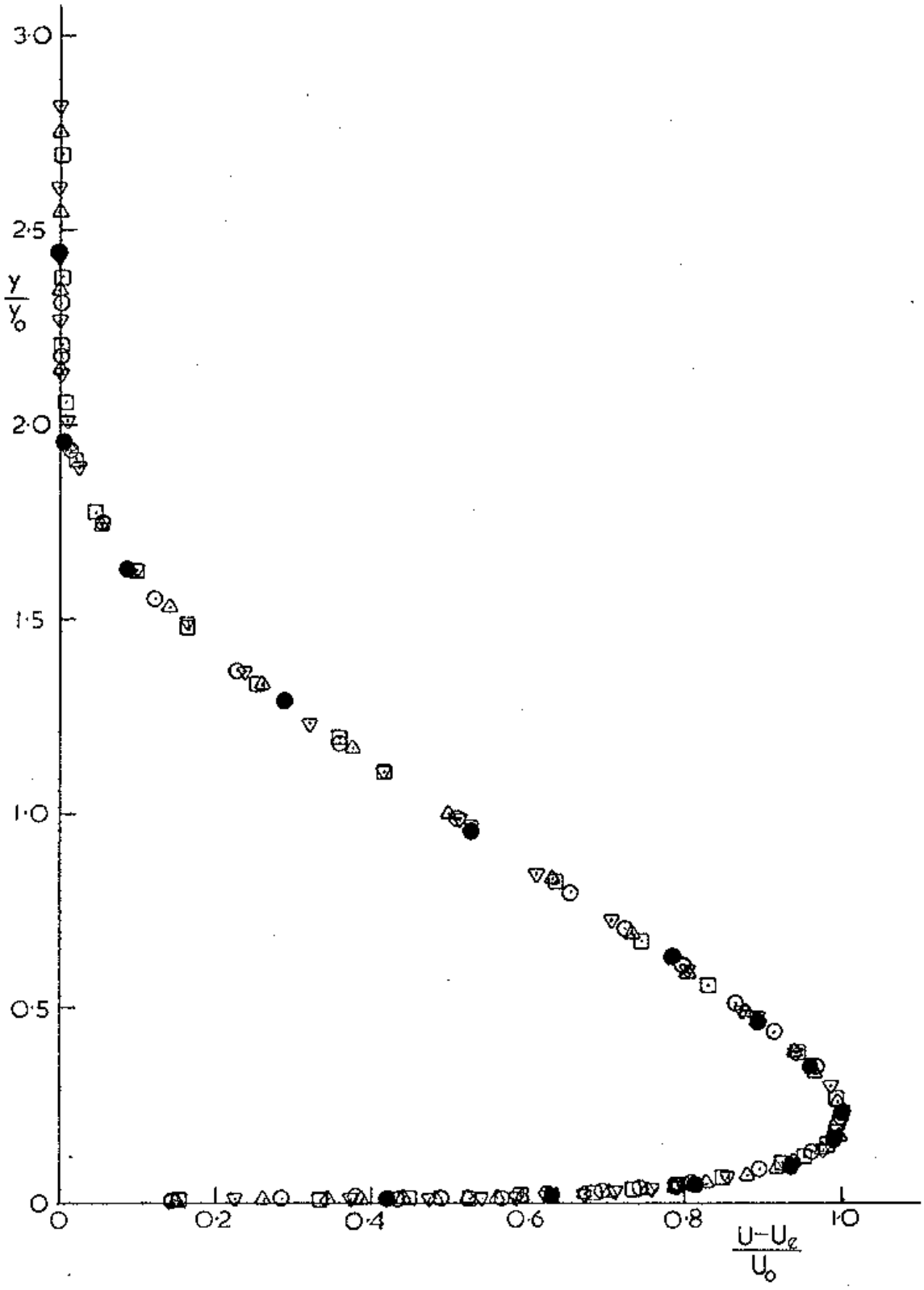

Fig. 8 Mean Velocity Profiles. Hot Wire Data ⊙, ⊡, ▽, △, x/b = 82.2, 139.5, 194.0, 248.0 respectively; Pitot Tube Data ● ;x/b = 251.0.

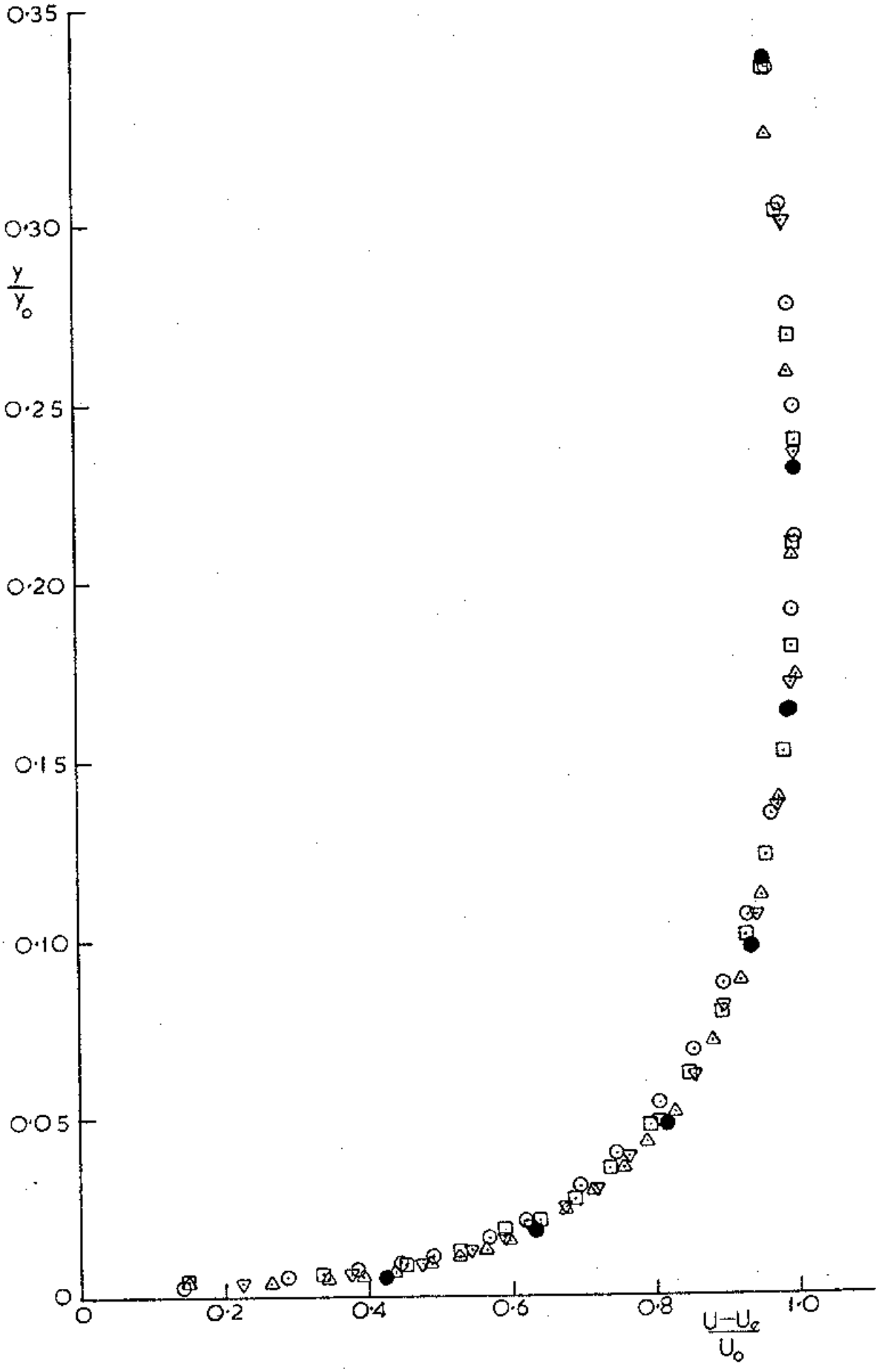

Fig. 9. Mean Velocity Profile in Inner Region. Hot Wire Data ⊙,⊡,▽,△ x/b = 82.2, 139.5, 194.0, 248.0 respectively; Pitot Tube Data ● x/b = 251.0.

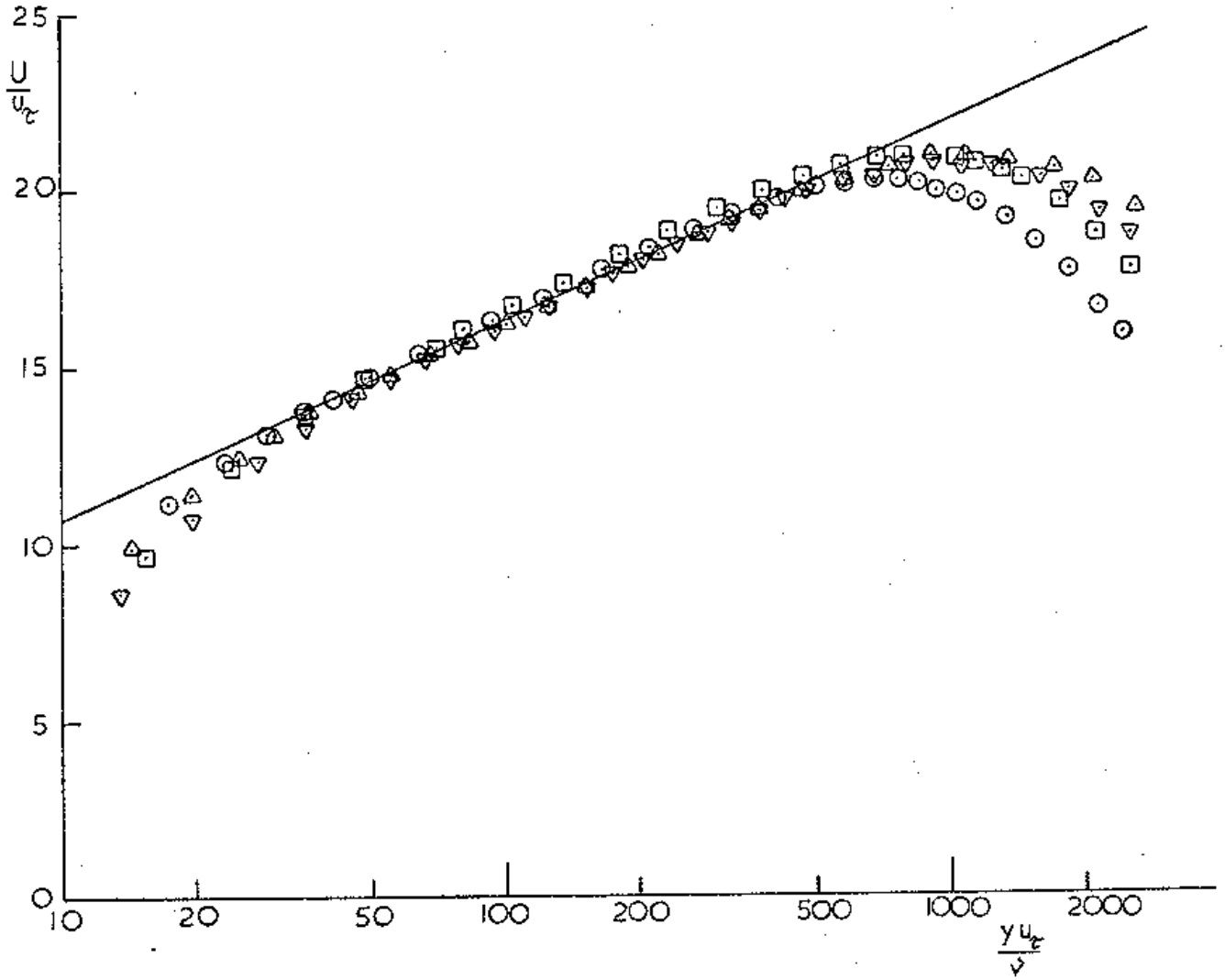

Fig. 10 Semi-logarithmic Plot of Mean Velocity in the Wall Region. Hot Wire Data $U_m Y_m$ ○,□,▽,△, x/b = 82.2, 139.5, 194.0, 248.0 and $\frac{U_m Y_m}{\nu} \times 10^{-4}$ = 1.37, 1.77, 2.15, 2.42 respectively: ——— Law of the Wall According to Patel (1965).

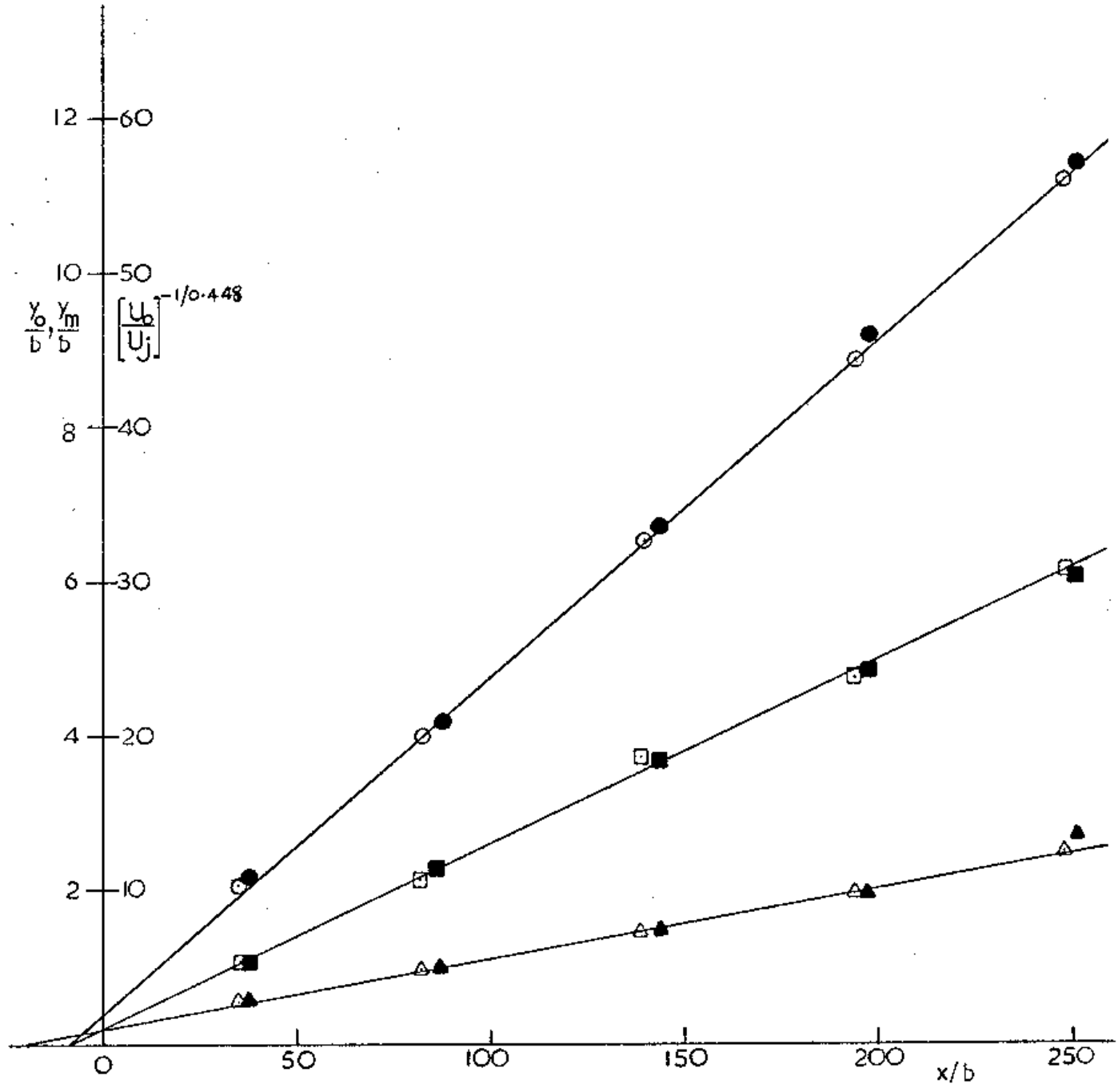

Fig. 11 Variation of Length and Velocity Scales. Hot Wire Data ⊙, △, ⊡, $\frac{y_0}{b}$, $\frac{y_m}{b}$, $\left[\frac{U_0}{U_J}\right]^{-1/.448}$ respectively:

Pitot Tube Data ●, ▲, ■ .

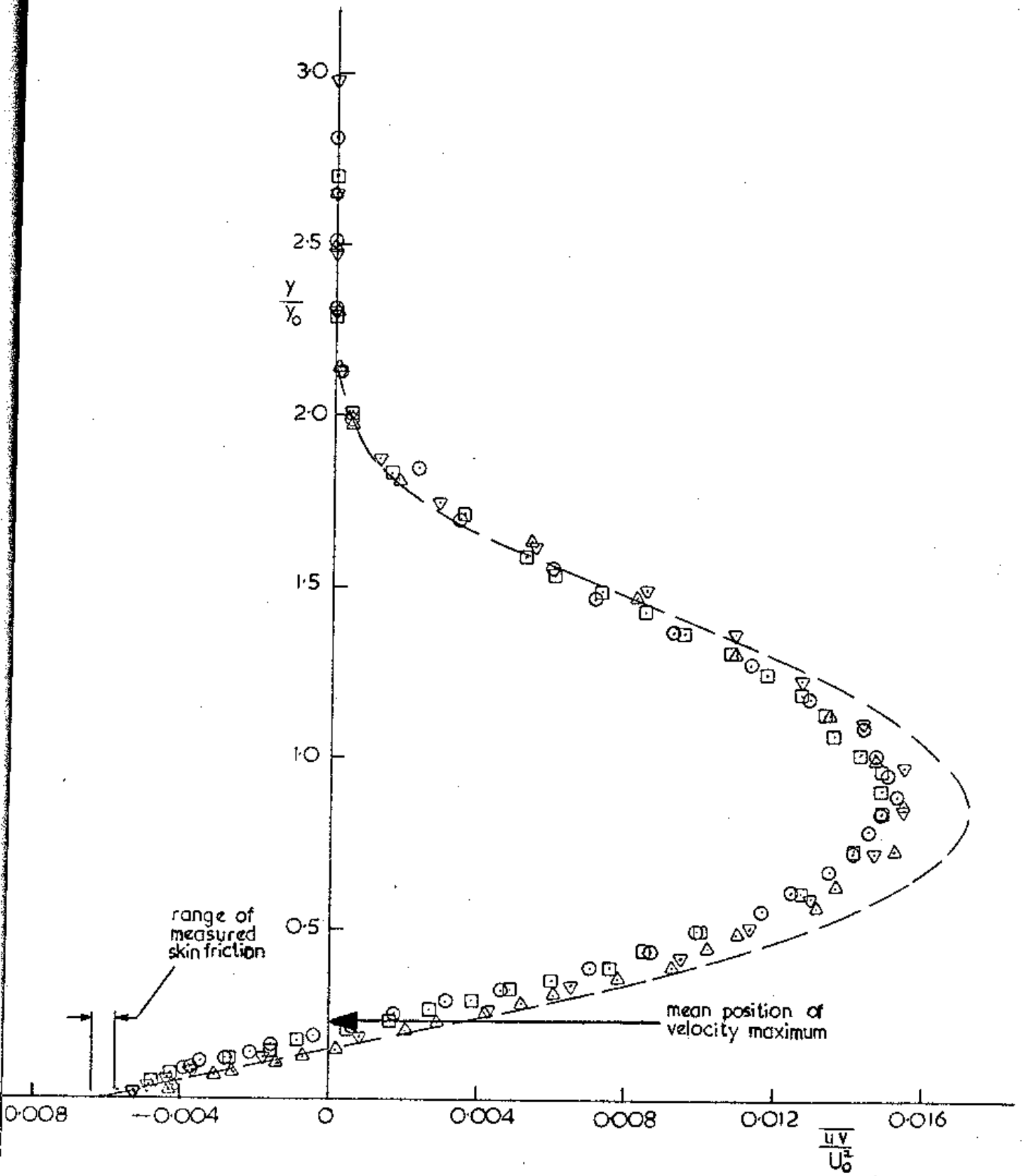

Fig. 12 Distribution of $\overline{uv}$ Across Wall Jet. ⊙,⊡,▽,△, Hot Wire Measurements at x/b = 82.2, 139.5, 194.0, 248.0 respectively. ----- Calculated From the Mean Momentum Equation.

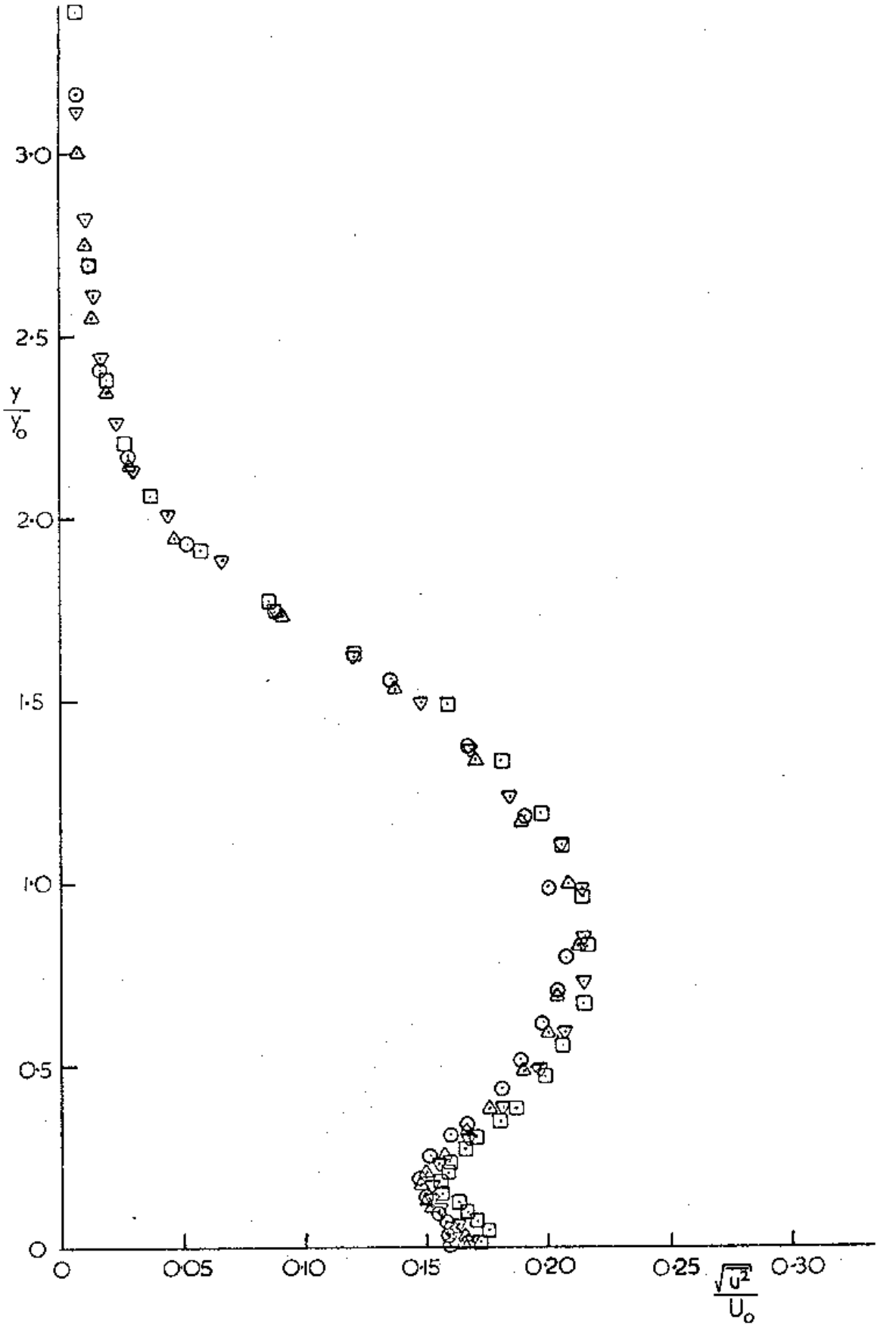

Fig. 13 Distribution of $\overline{u^2}$ Across Wall Jet. ⊙,⊡,▽,△, x/b = 82.2, 139.5, 194.0, 248.0 respectively.

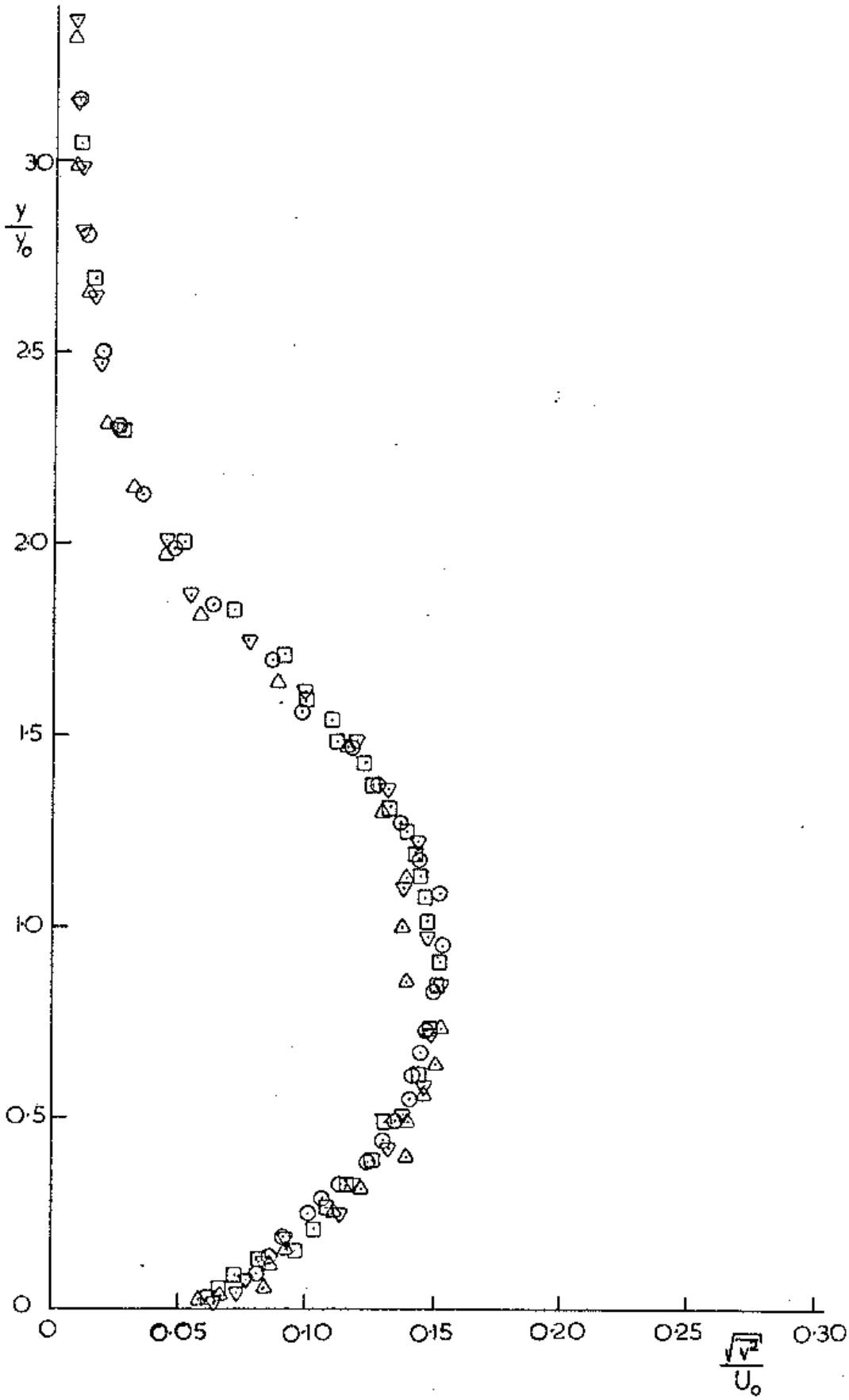

Fig. 14 Distribution of $\overline{v^2}$ Across Wall Jet. ⊙,⊡,▽,△, x/b = 82.2, 139.5, 194.0, 248.0 respectively.

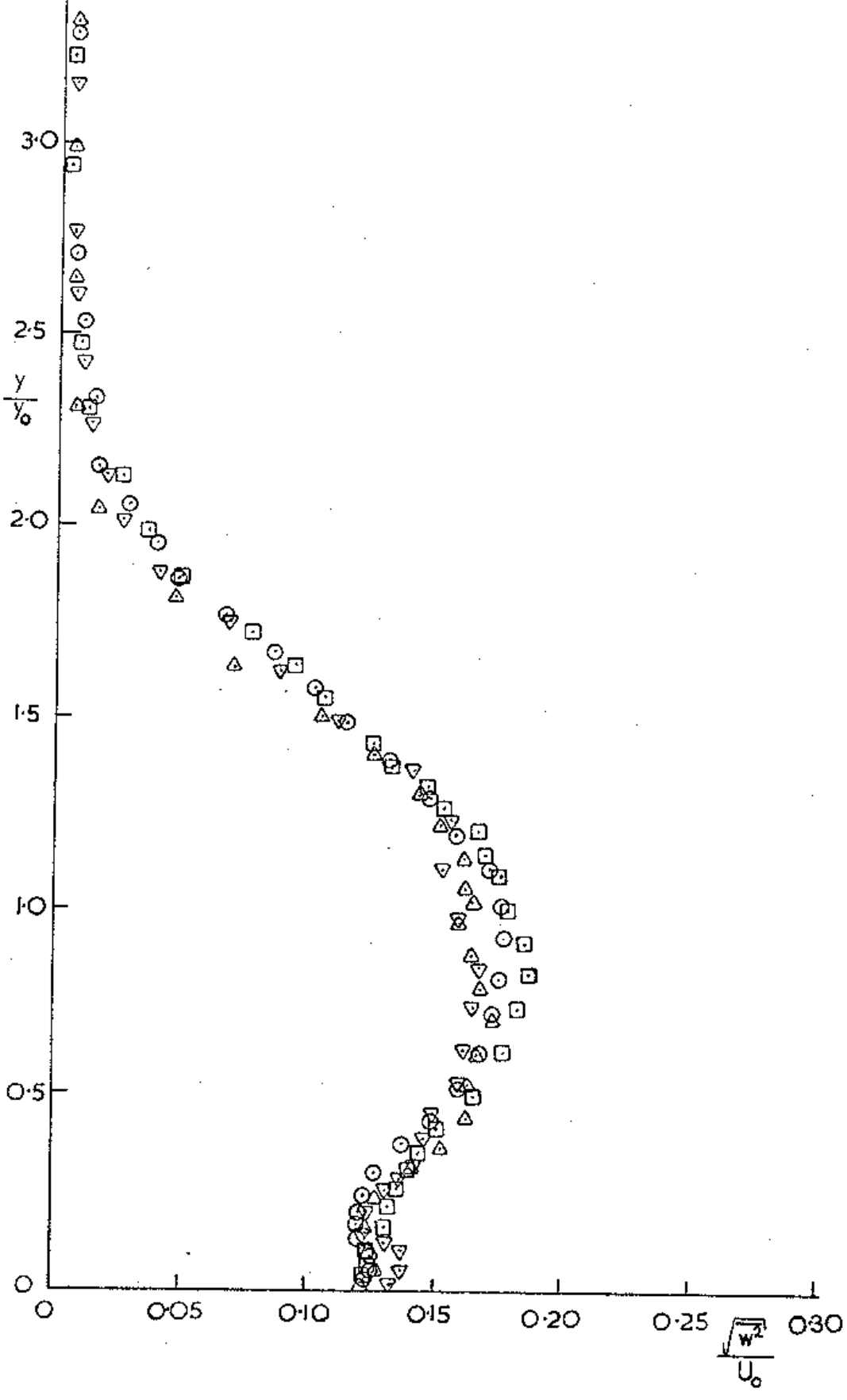

Fig. 15 Distribution of $\overline{w^2}$ Across Wall Jet. ⊙,⊡,▽,△, x/b = 82.2, 139.5, 194.0, 248.0 respectively.

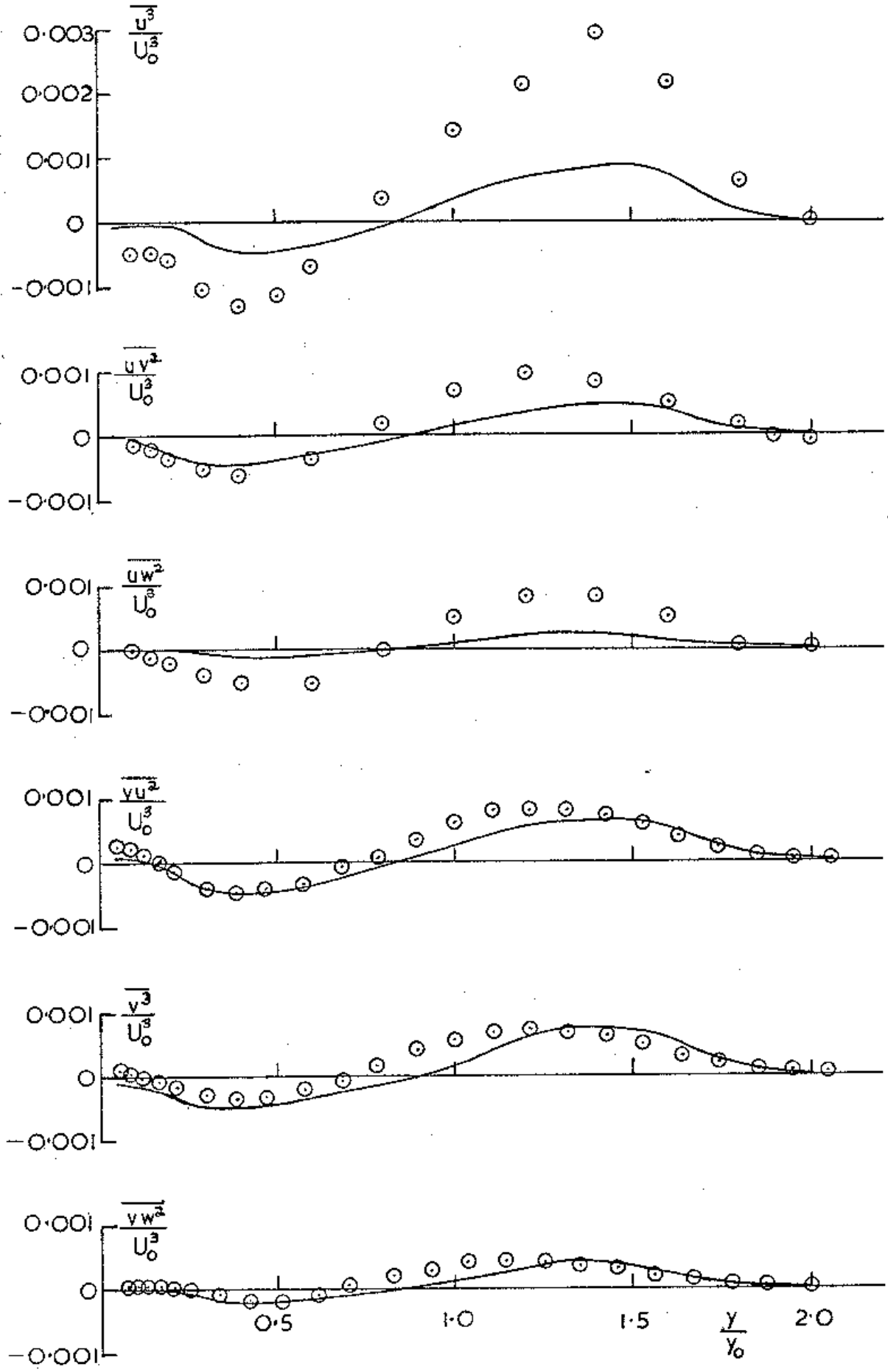

Fig. 16 Distribution of Triple Velocity Correlations Across Wall Jet. ⊙ Measured Values x/b = 194.0, ———— Model of Hanjalic and Launder (1972(b)) (Equations 22).

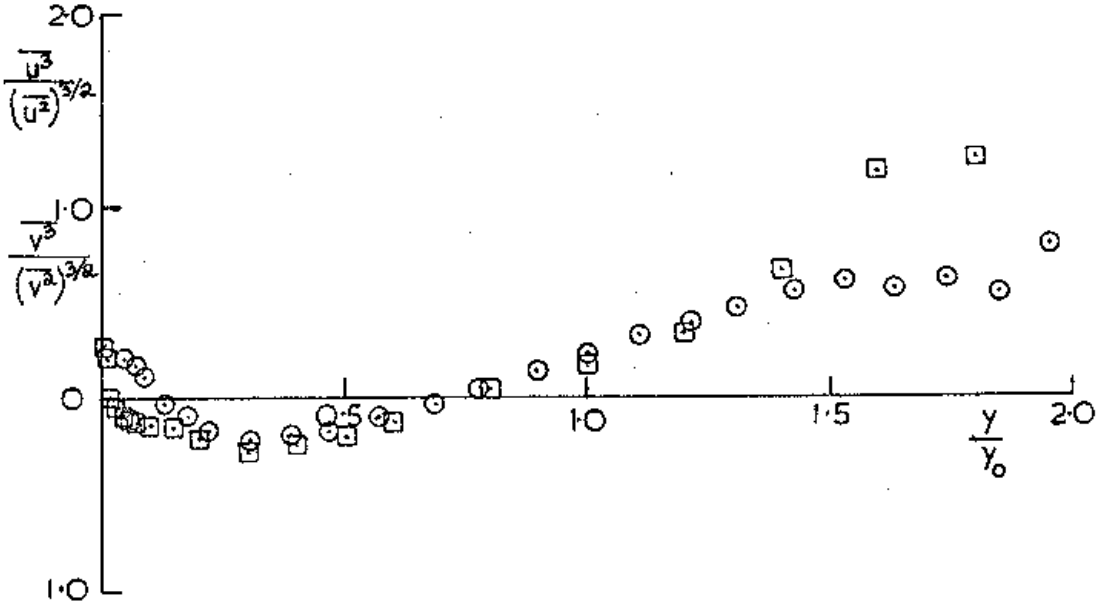

Fig. 17 Skewness Factors of u and v. ⊡, ⊙, Skewness of u and v respectively. x/b = 194.0.

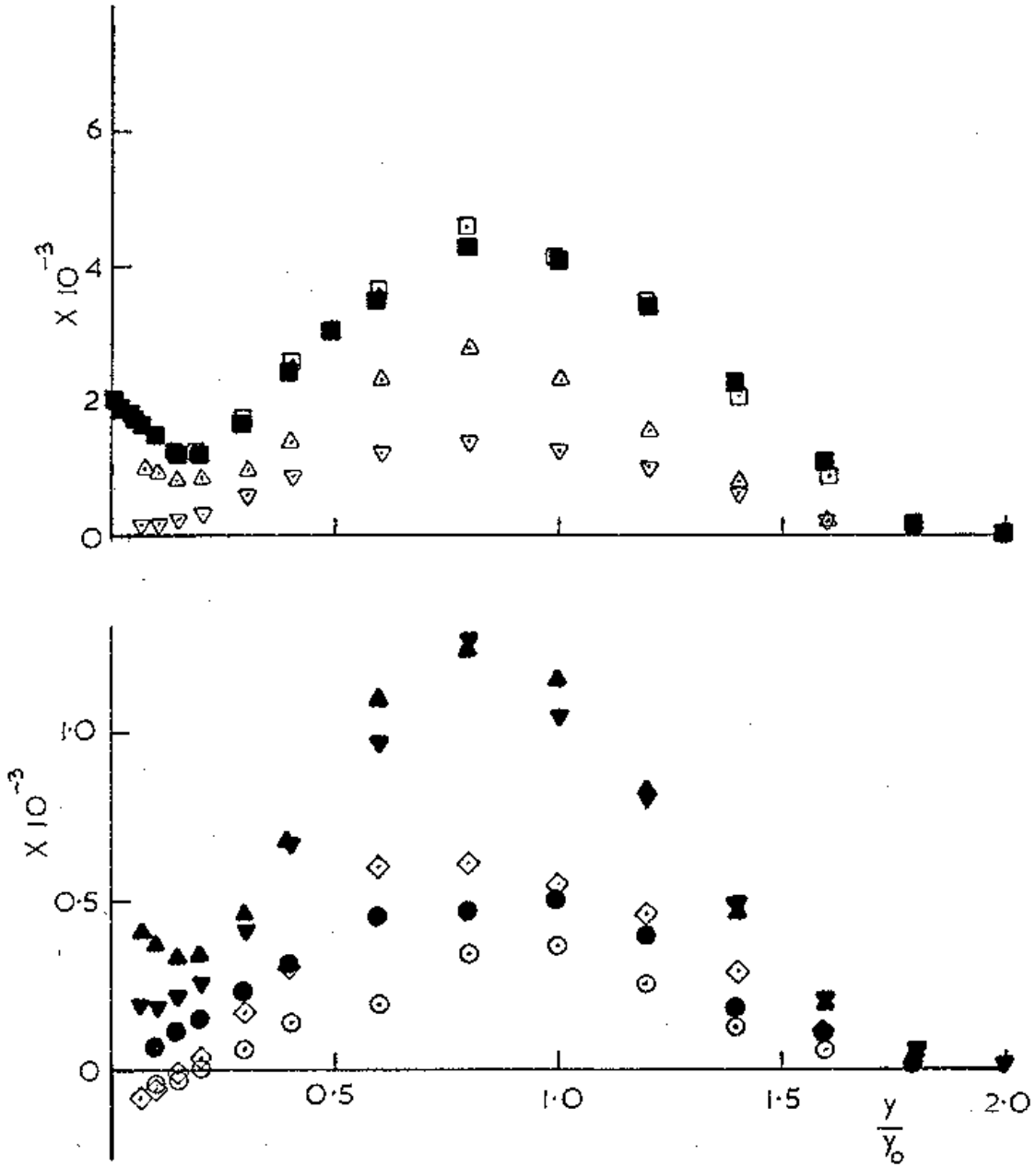

Fig. 18 Quadruple Velocity Correlations. (a) Single Normal Wire ■ u^4/U_0^4; X-Wire ⊡, ▽, △ $\overline{u^4}/U_0^4$, $\overline{v^4}/U_0^4$ and $\overline{w^4}/U_0^4$ respectively: (b) X-Wire ▼, ▲, ●, ◇, ⊙, $\overline{u^2v^2}/U_0^4$, $\overline{u^2w^2}/U_0^4$, $\overline{v^2w^2}/U_0^4$ $\overline{uv^3}/U_0^4$ and $\overline{uvw^2}/U_0^4$ respectively. x/b = 194.0..

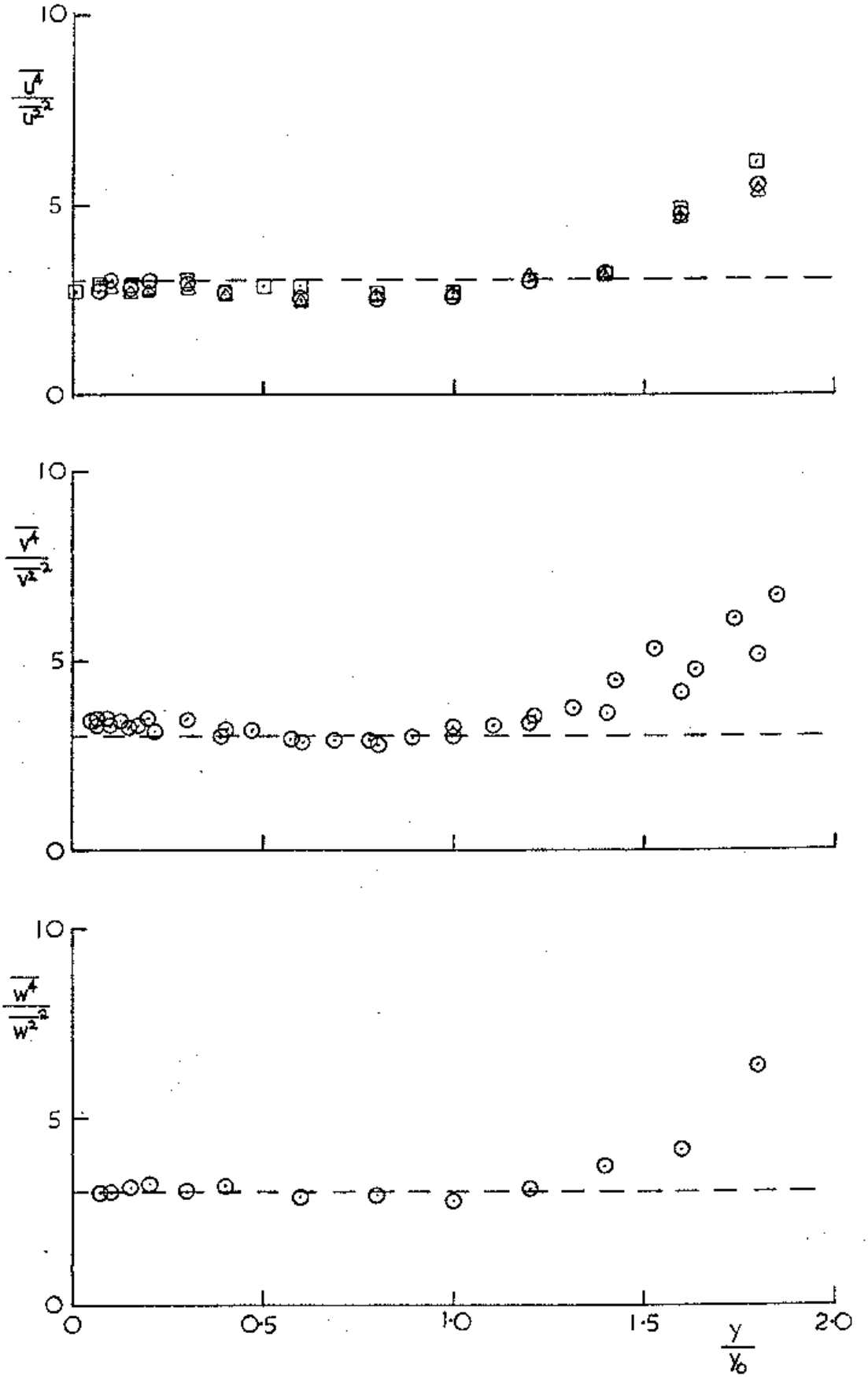

Fig. 19 Flatness Factors. ----- Gaussian Value: For $\overline{u^4}/\overline{u^2}^2$ ⊡ Normal Wire, ⊙ X-Wire in Vertical Plane, △ X-Wire in Horizontal Plane. x/b = 194.0.

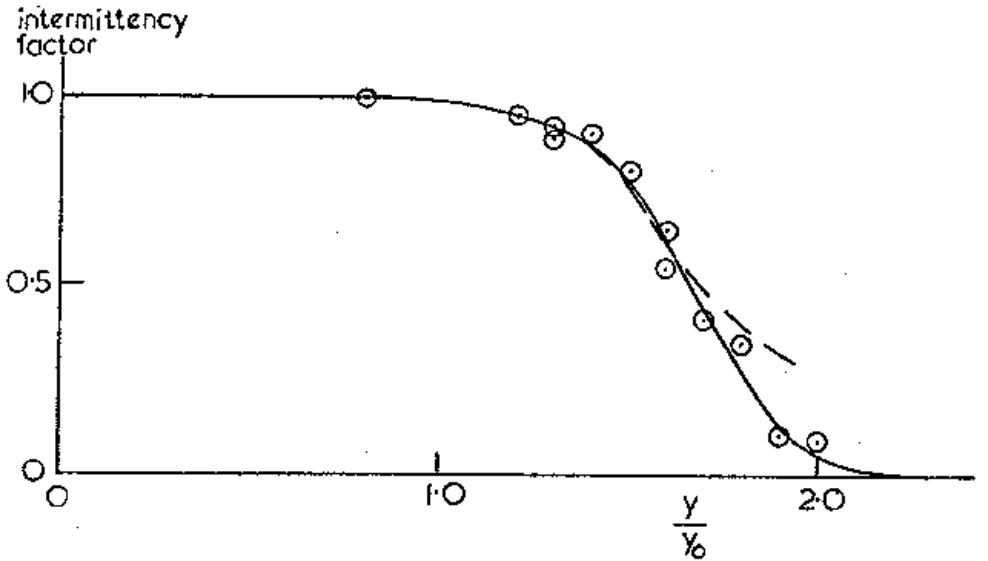

Fig. 20 Intermittency Measurements. —⊙— From Mirror Galvanometer Traces; ----- From Flatness Factor of u. x/b = 194.0.

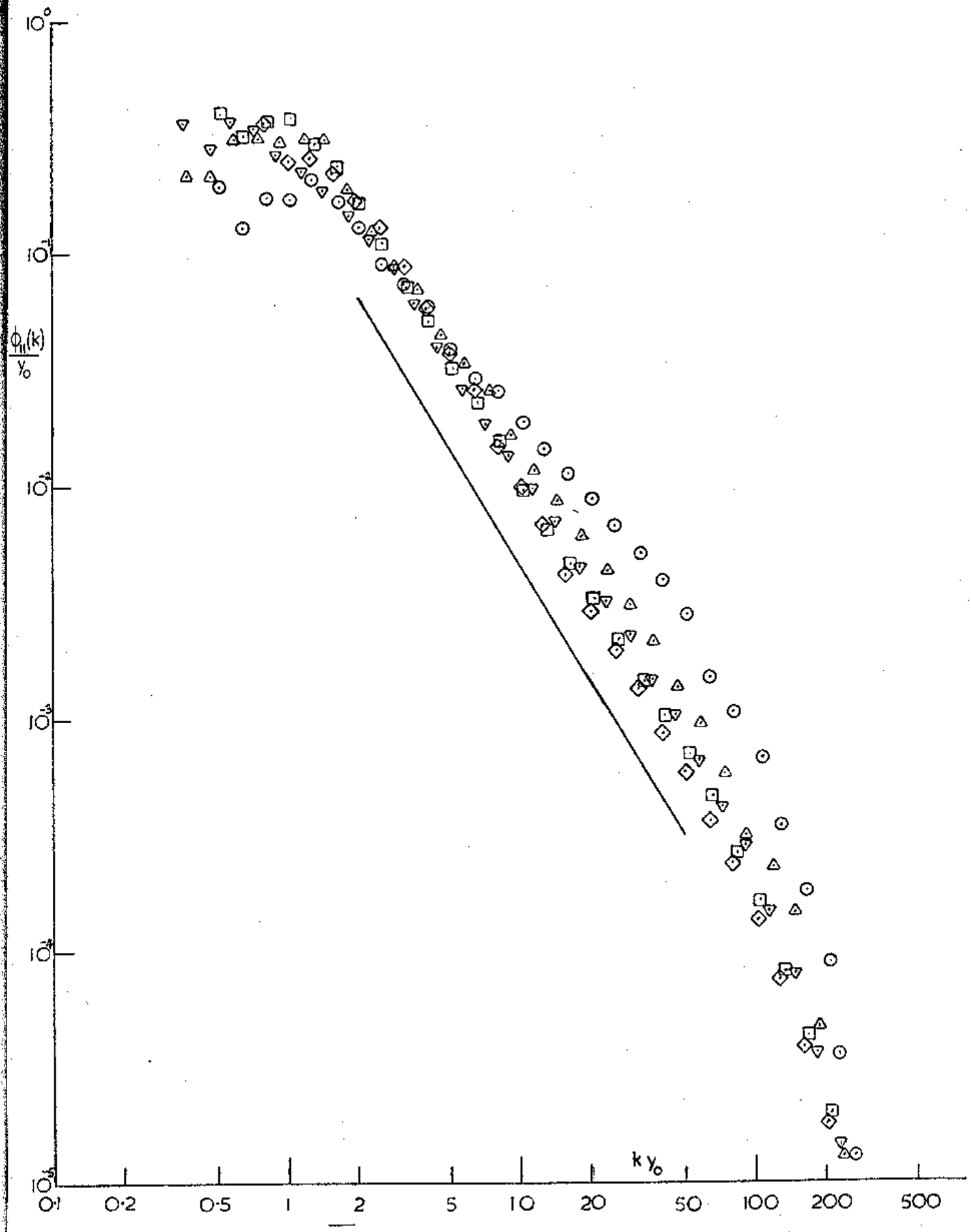

Fig. 21 Spectra of $\overline{u^2}$ at Different Positions Across Wall Jet. ⊙,△,▽,⊡,◇, y/y_0 = 0.0084, 0.084, 0.24, 1.0 and 1.6 respectively, ——— Slope of -5/3 Law. x/b = 194.0.

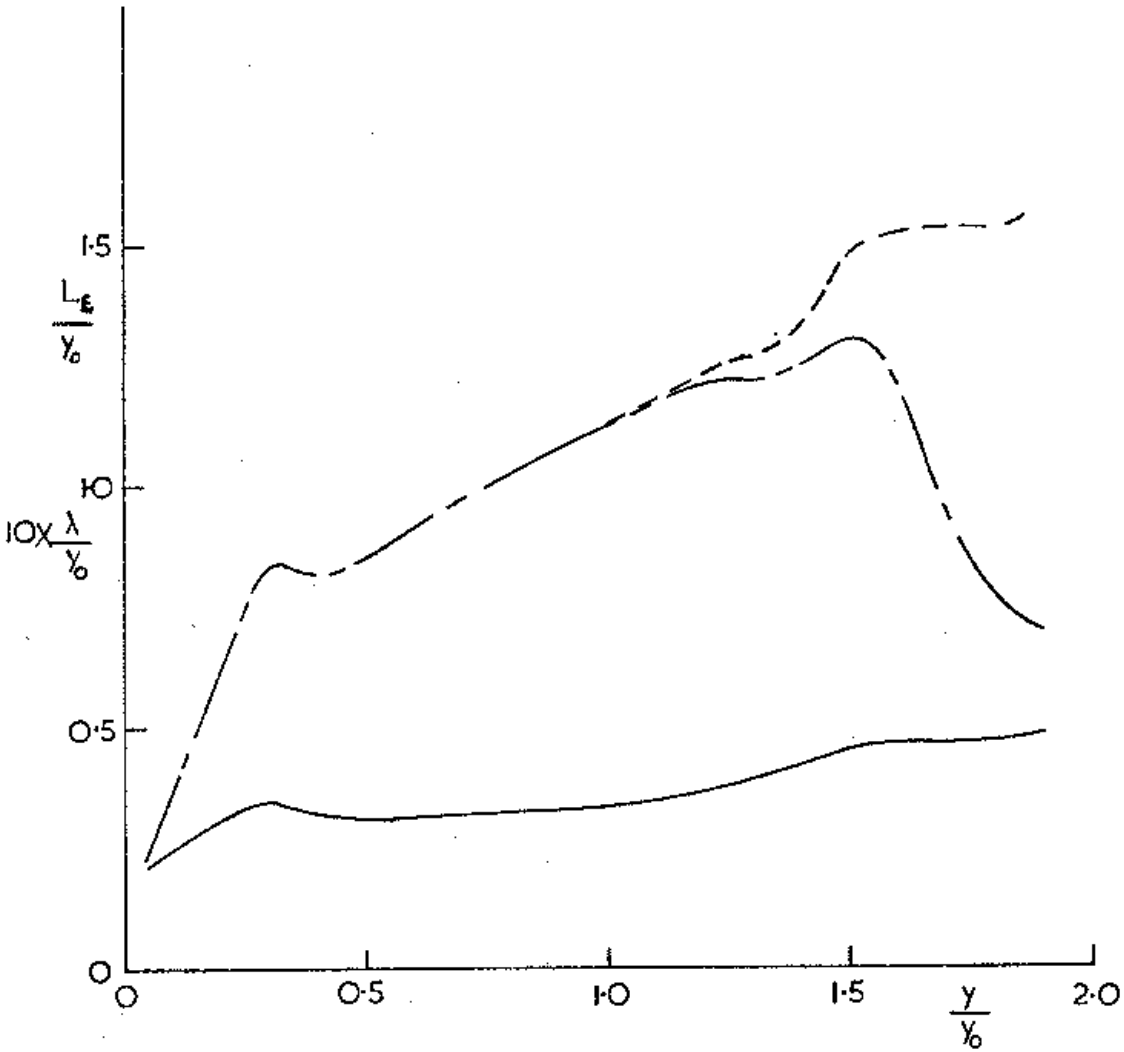

Fig. 22 Microscale and Dissipation Length Scale. ——— λ/y_0, ——— – ——— L_ε/y_0, ----- L_ε/y_0 Within Turbulent Fluid. x/b = 194.0.

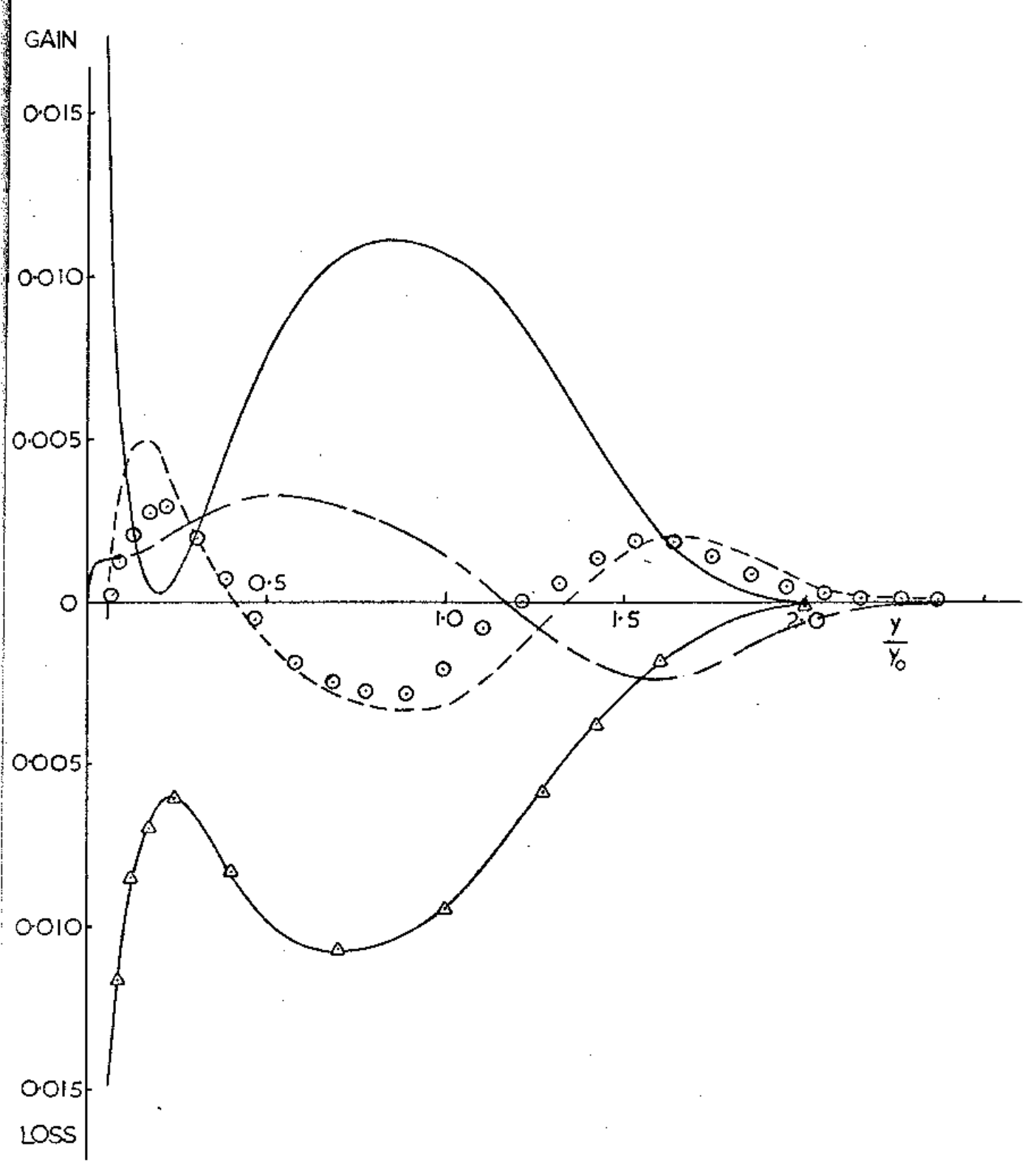

Fig. 23 Turbulence Energy Balance. ——— – ——— Advection, ——— Production, -----Total Diffusion (By Difference), ⊙ 'Velocity' Diffusion (Measured), ——— △ ——— Dissipation. x/b = 194.0.

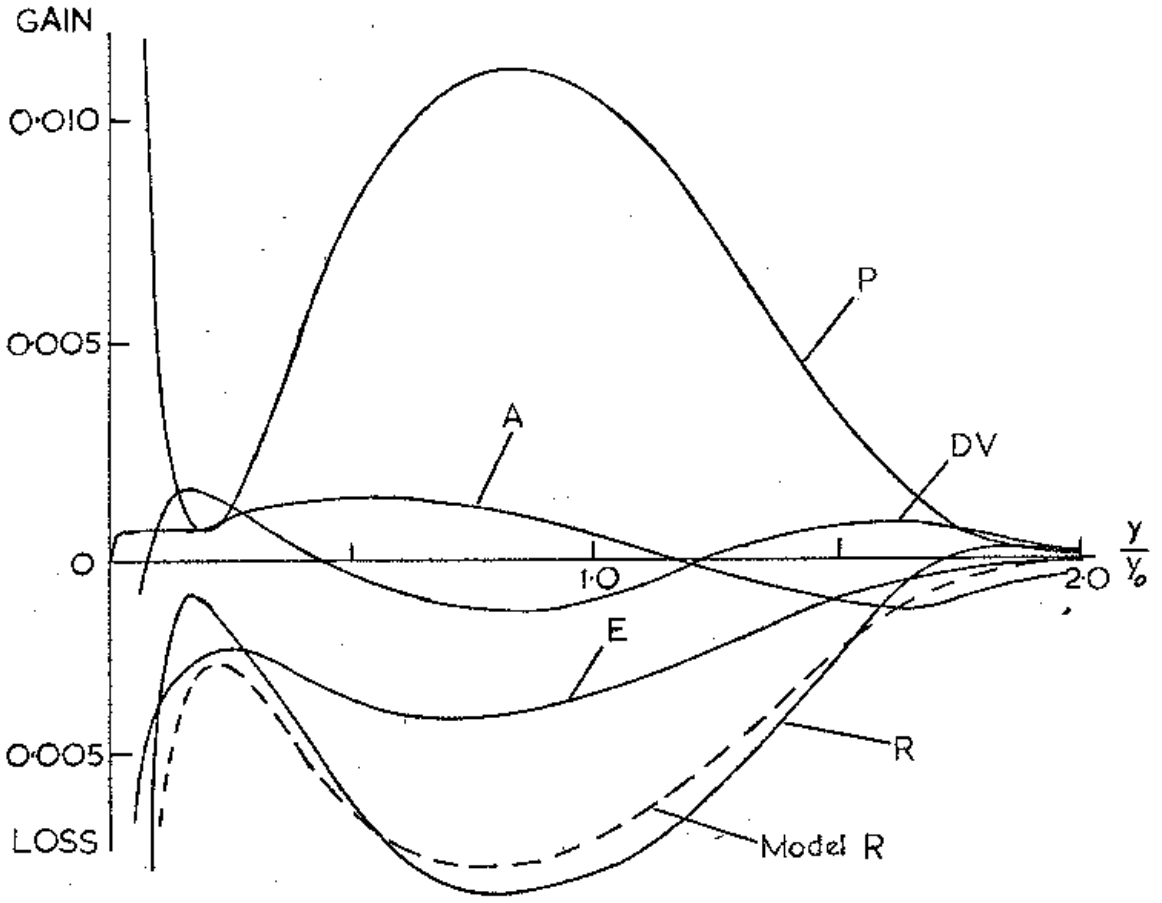

Fig. 24(a) Terms in the Equation for $\overline{u^2}$. A ≡ Advection, R ≡ Redistribution, P ≡ Production, DV ≡ Velocity Diffusion, E ≡ Dissipation, ----- Model of R According to Hanjalic and Launder (1972(b)).

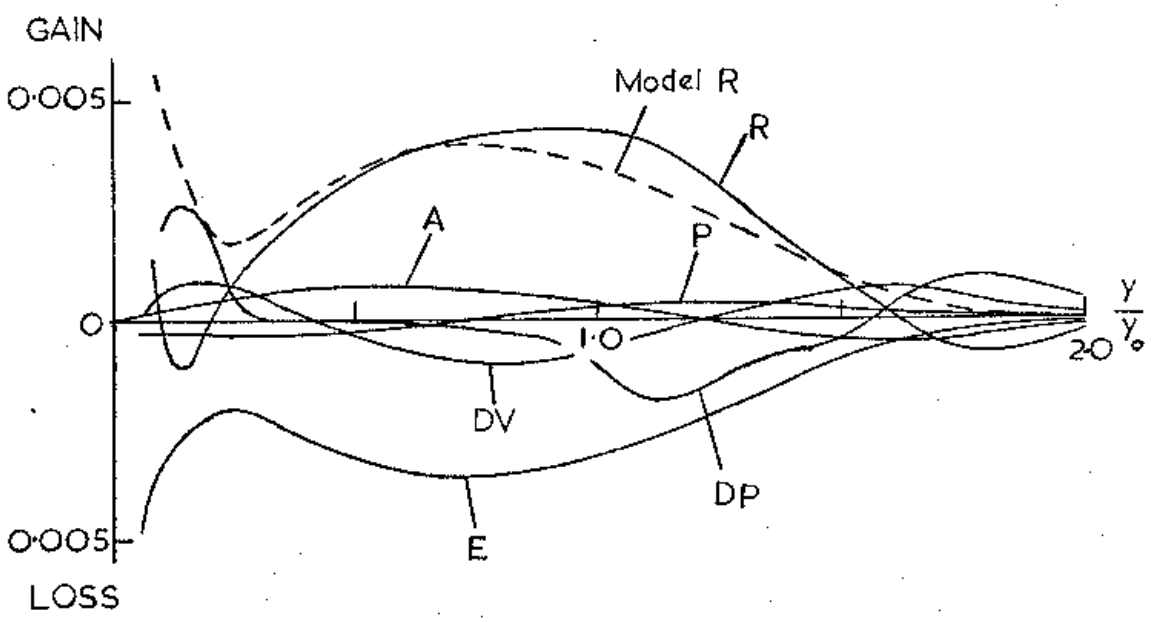

Fig. 24(b) Terms in the Equation for $\overline{v^2}$. DP ≡ 'Pressure' Diffusion, Other Terms as for Fig. 24(a).

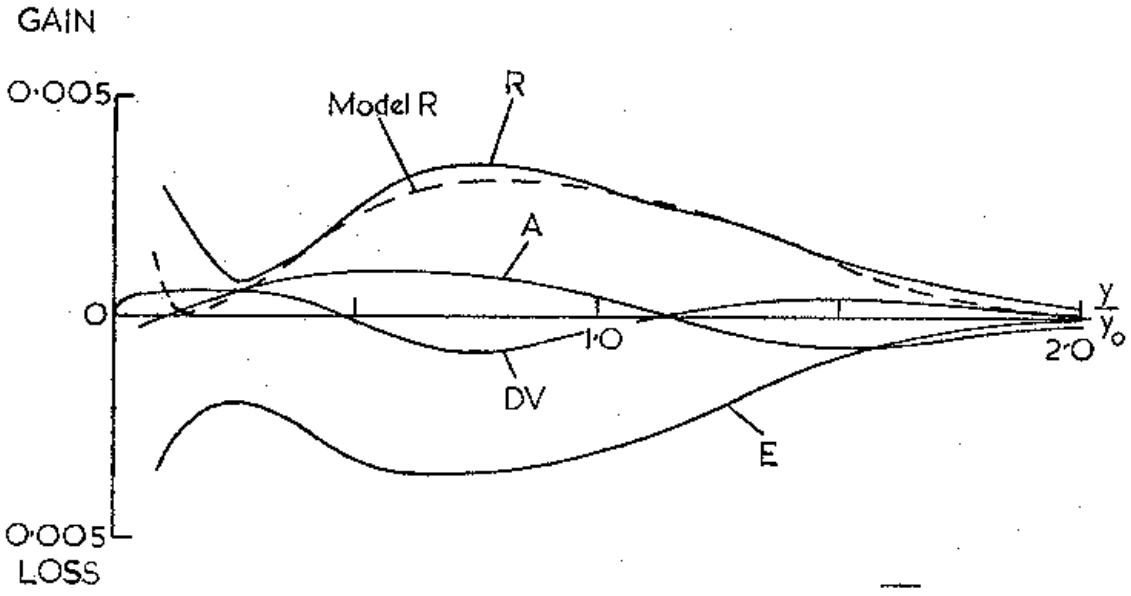

Fig. 24(c) Terms in the Equation for $\overline{w^2}$. Notation as in Fig. 24(a).

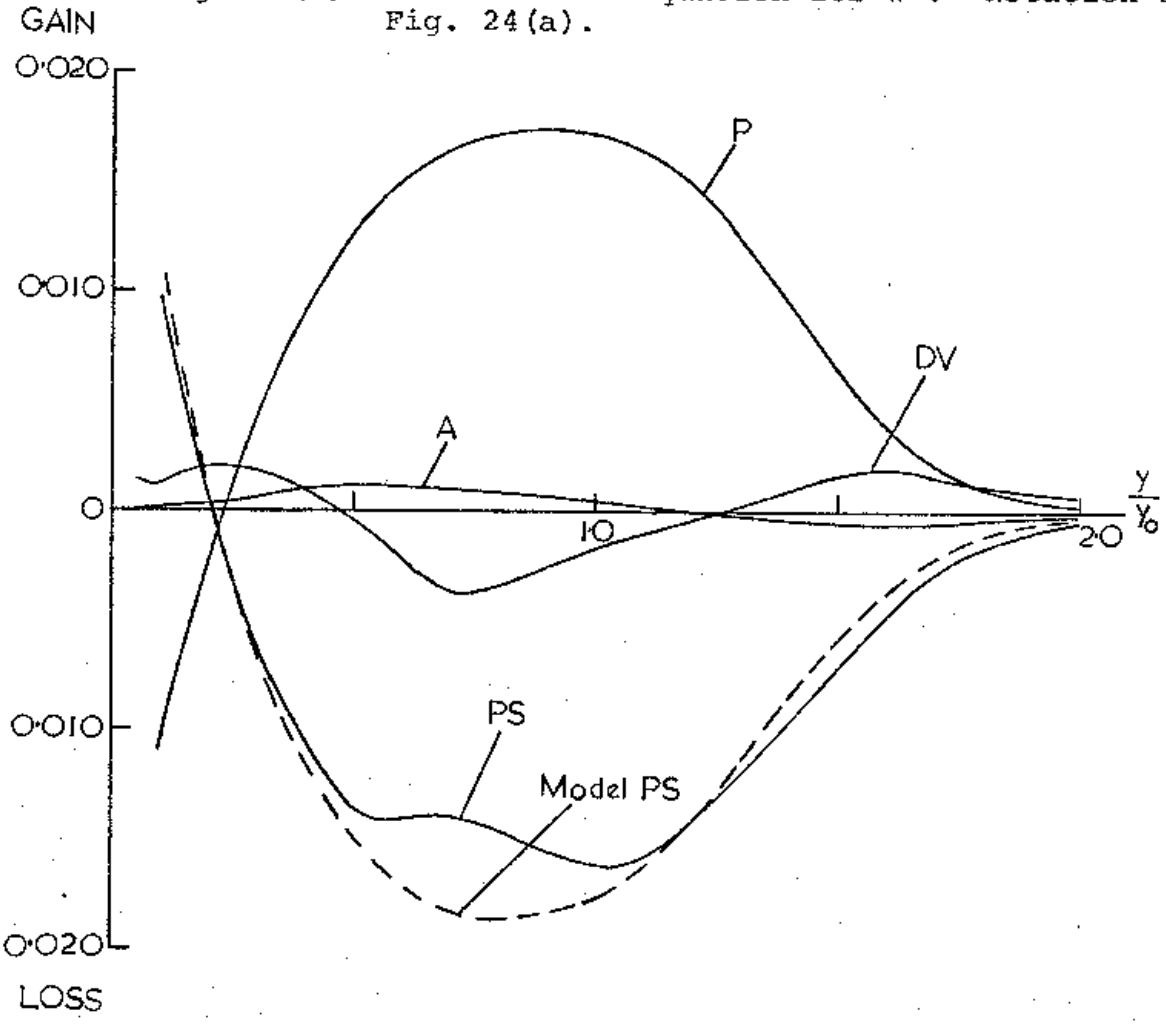

Fig. 24(d) Terms in Equation for $\overline{uv}$. PS ≡ Pressure Strain Correlation, ----- Model of PS According to Hanjalic and Launder (1972(b)), Remaining Notation as in Fig. 24(a).